

## Review Article

# Somatostatin receptor PET ligands - the next generation for clinical practice

Elin Pauwels<sup>1,2</sup>, Frederik Cleeren<sup>3</sup>, Guy Bormans<sup>3</sup>, Christophe M Deroose<sup>1,2</sup>

<sup>1</sup>Nuclear Medicine, University Hospitals Leuven, Leuven, Belgium; <sup>2</sup>Nuclear Medicine and Molecular Imaging, Department of Imaging and Pathology, KU Leuven, Leuven, Belgium; <sup>3</sup>Radiopharmaceutical Research, Department of Pharmacy and Pharmacology, KU Leuven, Leuven, Belgium

Received June 29, 2018; Accepted September 4, 2018; Epub October 20, 2018; Published October 30, 2018

**Abstract:** Somatostatin receptors (SSTRs) are variably expressed by a variety of malignancies. Using radiolabeled somatostatin analogs (SSAs), the presence of SSTRs on tumor cells may be exploited for molecular imaging and for peptide receptor radionuclide therapy. <sup>111</sup>In-DTPA-octreotide has long been the standard in SSTR scintigraphy. A major leap forward was the introduction of gallium-68 labeled SSAs for positron emission tomography (PET) offering improved sensitivity. Tracers currently in clinical use are <sup>68</sup>Ga-DOTA-Tyr<sup>3</sup>-octreotide (<sup>68</sup>Ga-DOTATOC), <sup>68</sup>Ga-DOTA-Tyr<sup>3</sup>-octreotate (<sup>68</sup>Ga-DOTATATE) and <sup>68</sup>Ga-DOTA-1-Nal<sup>3</sup>-octreotide (<sup>68</sup>Ga-DOTANOC), collectively referred to as <sup>68</sup>Ga-DOTA-peptides. <sup>68</sup>Ga-DOTA-peptide PET has superseded <sup>111</sup>In-DTPA-octreotide scintigraphy as the modality of choice for SSTR imaging. However, implementation of <sup>68</sup>Ga-DOTA-peptides in routine clinical practice is often limited by practical, economical and regulatory factors related to the use of the current generation of <sup>68</sup>Ge/<sup>68</sup>Ga generators. Centralized production and distribution is challenging due to the low production yield and relatively short half-life of gallium-68. Furthermore, gallium-68 has a relatively long positron range, compromising spatial resolution on modern PET cameras. Therefore, possibilities of using other PET radionuclides are being explored. On the other hand, new developments in SSTR PET ligands are strongly driven by the need for improved lesion targeting, especially for tumors with low SSTR expression. This may be achieved by using peptide vectors having a higher affinity for the SSTR or a broader affinity profile for the different receptor subtypes or by using compounds recognizing more binding sites, such as SSTR antagonists. This review gives an overview of recent developments leading to the next generation of clinical PET tracers for SSTR imaging.

**Keywords:** Somatostatin receptor, PET, SPECT, agonist, antagonist, DOTATATE, DOTATOC, DOTANOC, radionuclide

## Introduction and background

Somatostatin receptors (SSTRs) are G-protein coupled membrane receptors that were first described in rat pituitary tumor cells by Schonbrunn and Tashjian in 1978 [1]. Five different human subtypes have been identified, named SSTR1 to 5 [2]. While the genes for SSTR1, 3, 4 and 5 are intronless, the SSTR2 gene produces two splice variants, SSTR2A and B, differing only in the length of their cytoplasmic tail [3, 4]. SSTRs are expressed by a wide variety of normal human tissues, both in various regions of the brain and peripheral organs, such as the spleen, adrenals, pituitary gland, pancreas, liver, gastro-intestinal tract, kidneys and lungs, each exhibiting a characteristic expression pattern of the different SSTR sub-

types [5-8]. SSTRs have also been identified in several human tumor types. Neuroendocrine tumors (NETs) represent one of the groups with the highest incidence of SSTR expression [9]. For instance in gastroenteropancreatic (GEP) NETs, SSTRs are present in 80 to 100% of cases, except for insulinomas, which have a lower incidence of 50 to 70% [10]. Other NETs expressing SSTRs include pituitary adenomas, pheochromocytomas, paragangliomas, lung carcinoids, small-cell lung cancers, Merkel cell carcinomas, medullary thyroid carcinomas and neuroblastomas [11]. A wide variability in receptor density and subtype expression has been observed across the different NET types, but also within individual tumor types [9, 11]. In the majority of cases, SSTR2 is most abundant, even when other subtypes are present [8, 12].

## Next generation SSTR PET ligands

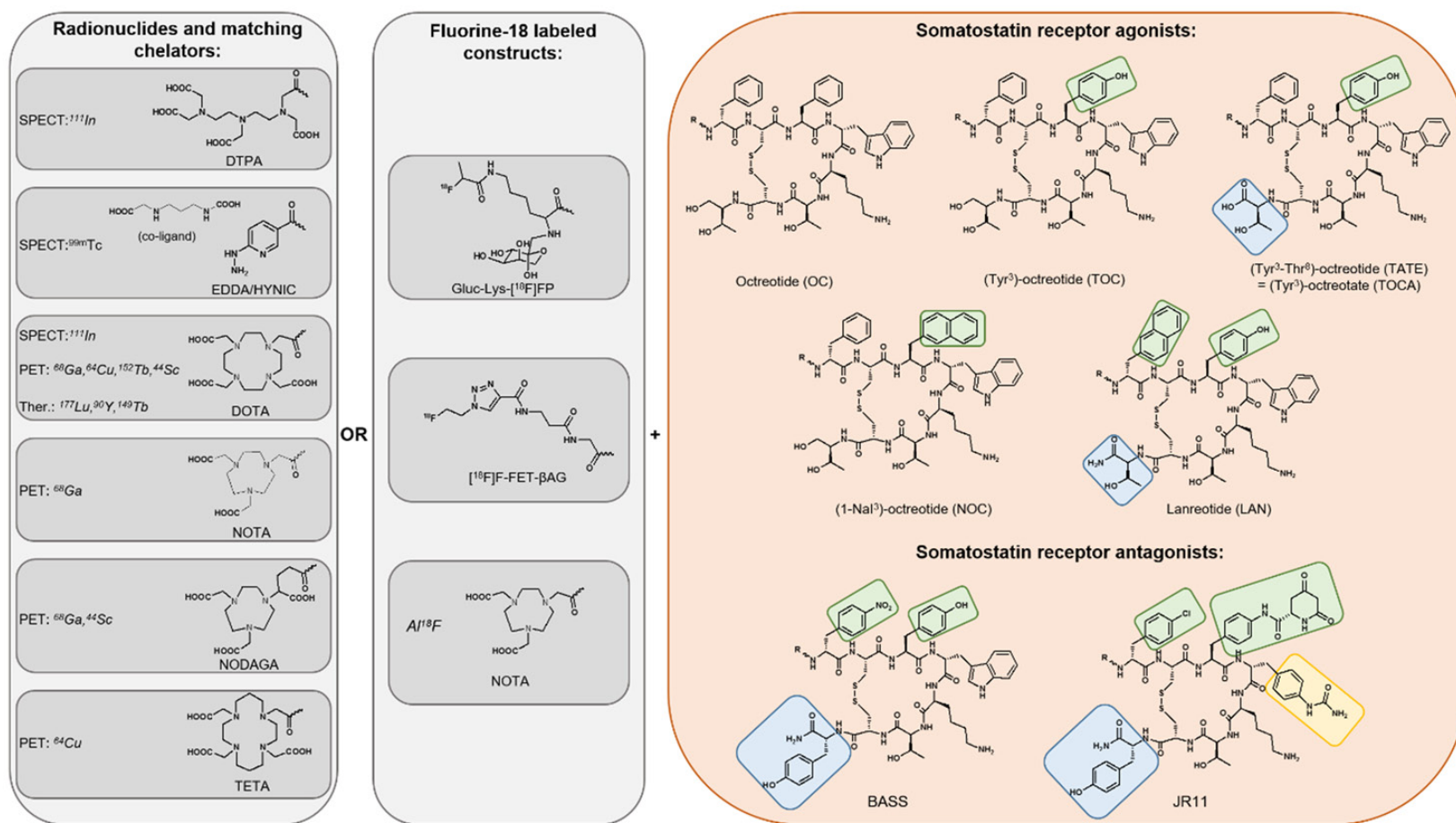


**Figure 1.** Chemical structures of the relevant SSTR tracers that have been applied in clinical practice or clinical studies: radionuclides with their matching chelators or fluorine-18 labeled constructs plus somatostatin receptor agonists or antagonists. (BASS: pNO<sub>2</sub>-Phe-c(D-Cys-Tyr-D-Trp-Lys-Thr-Cys)-D-TyrNH<sub>2</sub>; JR11: Cpa-c[D-Cys-Aph(Hor)D-Aph(Cbm)-Lys-Thr-Cys]-D-Tyr-NH<sub>2</sub>).

A large variety of other solid and hematological malignancies may also variably express SSTRs. These include meningiomas, gliomas, lymphomas, and breast, lung, renal cell, pancreato-biliary tract, liver cell, colorectal, ovarian and prostatic carcinomas [9, 11, 12].

The presence of SSTRs on tumor cells may open up an important window of opportunity for the clinical management of those tumors in terms of imaging and therapeutic options. Especially in NETs this opportunity has already been extensively exploited. SSTR overexpression is the foundation on which the use of somatostatin analogs (SSAs) such as octreotide in the pharmacological treatment of NETs is based [13]. According to the most recent European Neuroendocrine Tumor Society (ENETS) consensus guidelines, SSAs are indicated for symptom relief in case of functioning tumors that cause hormone production, as well as for tumor growth inhibition [14].

Furthermore, SSAs can be labeled with radionuclides. These radionuclides either have a heavy nucleus ( $Z > 83$ ) or possess an imbalance in proton/neutron ratio, or are in a metastable energy state and will undergo radioactive decay. The excess of energy in the nucleus of the unstable element can result in emission of either particles ( $\alpha$ ,  $\beta^{+/-}$ ) and/or electromagnetic radiation (gamma ray photons ( $\gamma$ )) and as a secondary effect X-rays, conversion electrons and Auger electrons. The specific decay characteristics of the radionuclide attached to the vector molecule determine if the radiopharmaceutical can be used for diagnostic (molecular imaging) or therapeutic (targeted radionuclide therapy) purposes. As such, SSTR imaging now occupies a key position in the clinical management of NETs [15-17]. Moreover, radiolabeling of SSTR targeting agents with therapeutic radionuclides may allow for vectorized radionuclide therapy, also called peptide receptor radionuclide therapy (PRRT). Currently, PRRT by means of radiolabeled SSAs represents an established, evidence-based treatment modality in case of inoperable/metastatic well-differentiated NETs [18] and its role has been enforced by the excellent results obtained in the randomized, controlled NETTER-1 trial [19].

In this review, we will focus on molecular imaging of the SSTR and more specifically on the

developments leading to the next generation of clinical PET tracers targeting the SSTR. Peptides can be radiolabeled with radiohalogens (e.g. iodine isotopes and fluorine-18) by standard carbon-halogen bond formation or with radiometals (e.g. indium-111 and gallium-68) using suitable bifunctional chelators that are covalently linked to the biologically active peptide [20]. Therefore, peptide-based radiopharmaceuticals typically consist of the vector moiety (the biologically active peptide) which is linked by means of a chelator, and possibly through an additional linker, to the radionuclide [21]. **Figure 1** shows the chemical structure of all relevant chelators discussed in this review with their matching radionuclides, in combination with the different SSAs that have been applied in clinical practice or clinical studies. Crucial for an effective SSTR tracer is its potential to bind the relevant SSTR [22]. It is important to realize that even small changes in the amino acid sequence of the peptide or a different choice of chelator or radionuclide might result in a different affinity profile [22, 23] (see also **Tables 1** and **2**). Recent advances in molecular imaging of the SSTR, relating to the choice of radionuclide and vectors molecules, will be discussed. **Figure 2** gives an overview of the likely future directions in the field of clinical SSTR PET imaging.

### From SPECT to PET. SSTR imaging: current status

SSTR imaging was first performed in humans in the late 1980s using  $^{123}\text{I}$ -Tyr<sup>3</sup>-octreotide [24]. However, due to several disadvantages such as a cumbersome radiolabeling procedure, high cost, limited availability of  $\text{Na}^{123}\text{I}$ , and considerable amount of intestinal accumulation of activity complicating interpretation of images, iodine-123 was soon replaced by indium-111, bound to the peptide by means of the chelator diethylenetriaminepentaacetic acid (DTPA) [25, 26].  $^{111}\text{In}$ -DTPA-octreotide (or  $^{111}\text{In}$ -pentetreotide) has long been the standard in SSTR imaging [22, 27]. Indium-111 is a  $\gamma$ -emitting radionuclide, thus imaging is performed by means of planar scintigraphy or single photon emission computed tomography (SPECT), with or without computed tomography (CT). However, there are some drawbacks to the use of indium-111, such as unfavorable nuclear physical characteristics resulting in suboptimal

## Next generation SSTR PET ligands

**Table 1.** *In vitro* affinity profile (50% inhibitory concentration ( $IC_{50}$ ) in nM  $\pm$  standard error of the mean) for the human somatostatin receptor of several somatostatin analogs

Somatostatin analog	SSTR1	SSTR2	SSTR3	SSTR4	SSTR5	Data from
Octreotide	> 10,000	2.0 $\pm$ 0.7	187 $\pm$ 55	> 1,000	22 $\pm$ 6	[23]
In-DTPA-octreotide	> 10,000	22 $\pm$ 3.6	182 $\pm$ 13	> 1,000	237 $\pm$ 52	[23]
Ga-DOTATATE	> 10,000	0.2 $\pm$ 0.04	> 1,000	300 $\pm$ 140	377 $\pm$ 18	[23]
Ga-DOTATOC	> 10,000	2.5 $\pm$ 0.5	613 $\pm$ 140	> 1,000	73 $\pm$ 12	[23]
Ga-DOTANOC	> 10,000	1.9 $\pm$ 0.4	40 $\pm$ 5.8	260 $\pm$ 74	7.2 $\pm$ 1.6	[35]
Gluc-Lys-FP-TOCA	> 10,000	2.8 $\pm$ 0.4	> 1,000	437 $\pm$ 84	123 $\pm$ 8.8	[125]
F-FET- $\beta$ AG-TOCA	NA	4.7	NA	8,600	NA	[69]
DOTA-Ianreotide	> 10,000	26 $\pm$ 3.4	771 $\pm$ 229	> 10,000	73 $\pm$ 12	[23]
Y-DOTA-Ianreotide	> 10,000	23 $\pm$ 5	290 $\pm$ 105	> 10,000	16 $\pm$ 3.4	[23]
Ga-KE88	9.5 $\pm$ 4.3	4.1 $\pm$ 1.4	2.7 $\pm$ 1.0	4.9 $\pm$ 1.4	2.25 $\pm$ 0.5	[102]
AM3	119 $\pm$ 6	2.3 $\pm$ 0.2	4.0 $\pm$ 0.03	97 $\pm$ 21	27 $\pm$ 1	[103]
DOTA-LTT-SS28	9.8 $\pm$ 0.2	2.5 $\pm$ 0.3	2.2 $\pm$ 0.5	4.8 $\pm$ 1.1	2.8 $\pm$ 0.3	[105]
In-DOTA-LTT-SS28	14 $\pm$ 1.2	1.8 $\pm$ 0.2	4.0 $\pm$ 0.2	5.4 $\pm$ 0.3	1.4 $\pm$ 0.2	[105]
DOTA-BASS	> 1,000	1.5 $\pm$ 0.4	> 1,000	287 $\pm$ 27	> 1,000	[110]
In-DOTA-BASS	> 1,000	9.4 $\pm$ 0.4	> 1,000	380 $\pm$ 57	> 1,000	[110]
NODAGA-JR11	> 1,000	4.1 $\pm$ 0.2	> 1,000	> 1,000	> 1,000	[114]
Ga-NODAGA-JR11	> 1,000	1.2 $\pm$ 0.2	> 1,000	> 1,000	> 1,000	[114]
DOTA-JR11	> 1,000	0.72 $\pm$ 0.12	> 1,000	> 1,000	> 1,000	[114]
Ga-DOTA-JR11	> 1,000	29 $\pm$ 2.7	> 1,000	> 1,000	> 1,000	[114]
Lu-DOTA-JR11	> 1,000	0.73 $\pm$ 0.15	> 1,000	> 1,000	> 1,000	[114]

Structures are explained in **Figure 1**, except for KE88 (DOTA-D-Dab-Arg-Phe-Phe-D-Trp-Lys-Thr-Phe), AM3 (DOTA-Tyr-cyclo(DAB-Arg-cyclo(Cys-Phe-D-Trp-Lys-Thr-Cys))) and SS28 (somatostatin-28).

**Table 2.**  $IC_{50}$  values (in nM  $\pm$  standard error of the mean (SEM)) from competitive binding assays in the rat pancreatic cancer cell line AR42J with high SSTR2 expression for several somatostatin analogs

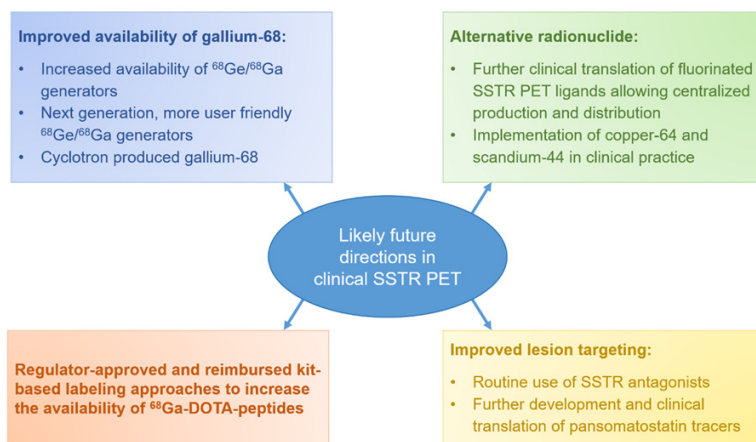
Somatostatin analog	$IC_{50} \pm$ SEM	Data from
In-DTPA-octreotide	6.3 $\pm$ 0.9	[74]
Ga-DOTATATE	0.20 $\pm$ 0.18	[86]
Ga-NOTA-octreotide	13 $\pm$ 3	[74]
AIF-NOTA-octreotide	3.6 $\pm$ 0.6	[74]
Sc-DOTATATE	0.70 $\pm$ 0.20	[86]

image quality and relatively high effective doses, limited availability and high costs [27, 28]. Successful efforts have been made to label SSAs with technetium-99m instead [27-29]. One of these compounds is  $^{99m}Tc$ -ethylene-diamine-N,N'-diacetic acid/hydrazinonicotinamide-Tyr<sup>3</sup>-octreotide ( $^{99m}Tc$ -EDDA/HYNIC-TOC) (see **Figure 1**), which is registered in Poland ( $^{99m}Tc$ -Tektrotyd; Polatom) and used in several mainly Eastern European countries.

A major leap forward was the introduction of SSAs labeled with the positron-emitting radio-

nuclide gallium-68 for positron emission tomography (PET) applications. This was made possible by the development of 1,4,7,10-tetraazacyclododecane-1,4,7,10-tetraacetic acid (DOTA), a macrocyclic chelator capable of forming stable complexes with a multitude of 2<sup>+</sup> and 3<sup>+</sup> charged radiometals [30, 31] that can be coupled to SSAs (see **Figure 1**). PET offers several advantages over SPECT, such as a higher sensitivity and spatial resolution and the possibility for straightforward image quantification [22]. The first clinical publication in this field reported on the use of  $^{68}Ga$ -DOTA-TOC ( $^{68}Ga$ -DOTATOC) in patients with meningiomas [32], closely followed by a publication on the application of  $^{68}Ga$ -DOTATOC in NET patients [33], both in 2001. Since then,  $^{68}Ga$ -labeled SSA PET has rapidly emerged as an established technique for SSTR imaging, especially in NETs where it represents the molecular imaging modality of choice [17, 34]. Tracers currently in clinical use are  $^{68}Ga$ -DOTATOC,  $^{68}Ga$ -DOTA-Tyr<sup>3</sup>-octreotate ( $^{68}Ga$ -DOTATATE) and  $^{68}Ga$ -DOTA-1-Nal<sup>3</sup>-octreotide ( $^{68}Ga$ -DOTANOC), collectively referred to as  $^{68}Ga$ -DOTA-peptides (see **Figure 1**).

## Next generation SSTR PET ligands



**Figure 2.** Overview of the likely future directions in the field of clinical SSTR PET imaging.

**Table 1** shows the affinity profiles, determined by means of *in vitro* binding studies, of most of the SSTR PET ligands discussed in this review as compared to  $^{111}\text{In}$ -DTPA-octreotide and octreotide. All listed  $^{68}\text{Ga}$ -DOTA-peptides show higher affinity for SSTR2 than  $^{111}\text{In}$ -DTPA-octreotide [23, 35]. Therefore, in tumors where SSTR2 is the most overexpressed subtype, such as NETs, this offers an additional benefit on top of the physical advantages associated with PET. As such, smaller lesions as well as lesions with low-to-moderate SSTR expression can be detected using  $^{68}\text{Ga}$ -DOTA-peptide PET imaging versus  $^{111}\text{In}$ -DTPA-octreotide SPECT [15]. Indeed, several studies comparing both techniques in a head-to-head manner consistently reported a superior performance of  $^{68}\text{Ga}$ -DOTA-peptide PET in NET patients [36-44] (see **Table 3**). An example is shown in **Figure 3**. An additional advantage is the fact that  $^{68}\text{Ga}$ -DOTATATE and  $^{68}\text{Ga}$ -DOTATOC are the theranostic twins of  $^{177}\text{Lu}$ -DOTATATE and  $^{90}\text{Y}$ -DOTATOC, currently the most frequently used radiopharmaceuticals for PRRT, and are as such ideally suited to identify eligible patients [45].

The affinity profiles of the  $^{68}\text{Ga}$ -DOTA-peptides show some differences (see **Table 1**), with the most prominent being the fact that  $^{68}\text{Ga}$ -DOTANOC also has high affinity for SSTR5 and to a lesser extent for SSTR3, while  $^{68}\text{Ga}$ -DOTATOC shows some affinity towards SSTR5 and  $^{68}\text{Ga}$ -DOTATATE only binds to SSTR2 [23, 35]. On the other hand, the affinity of  $^{68}\text{Ga}$ -DOTATATE for SSTR2 is an order of magnitude higher than that of the other  $^{68}\text{Ga}$ -DOTA-peptides.

Therefore, some differences in lesion detection rate might be expected. A meta-analysis regarding the diagnostic role of  $^{68}\text{Ga}$ -DOTATOC and  $^{68}\text{Ga}$ -DOTATATE reported a high sensitivity (93% and 96%, respectively) and specificity (85% and 100%, respectively) for both tracers [46]. A head-to-head comparison of  $^{68}\text{Ga}$ -DOTATOC and  $^{68}\text{Ga}$ -DOTATATE in 40 NET patients showed a comparable diagnostic accuracy, although significantly fewer lesions were detected with the latter (262 vs. 254) [47]. In a similar head-to-head

comparison of  $^{68}\text{Ga}$ -DOTATATE and  $^{68}\text{Ga}$ -DOTANOC in 20 NET patients, a comparable diagnostic accuracy was found as well with both tracers, with a slight, but not statistically significant difference in the number of detected lesions (130 vs. 116) [48]. Conversely, in another comparison study in 18 GEP NET patients,  $^{68}\text{Ga}$ -DOTANOC PET detected significantly more lesions than  $^{68}\text{Ga}$ -DOTATATE (238 vs. 212 out of 248 lesions), but the authors state that the clinical relevance of this observation has to be confirmed in larger trials [49]. Currently, there is no recommendation on which type of  $^{68}\text{Ga}$ -DOTA-peptide is preferred [17, 34, 50] and logistic reasons such as availability of the precursor peptide will guide the choice in clinical practice. Moreover, there are some practical obstacles to the implementation of  $^{68}\text{Ga}$ -DOTA-peptide PET that may differ from country to country. Examples are lack of  $^{68}\text{Ge}/^{68}\text{Ga}$  generators registered or cleared for human use, no availability of precursor peptide for human use, no reimbursement or the implementation is economically not viable.

### Radionuclide

Gallium-68 has the theoretical advantage that it is available from  $^{68}\text{Ge}/^{68}\text{Ga}$  generators and as such cyclotron independent. However, despite the excellent results achieved with  $^{68}\text{Ga}$ -DOTA-peptides, their use in routine clinical practice is often limited to large nuclear medicine departments. Unlike the  $^{99}\text{Mo}/^{99\text{m}}\text{Tc}$  generator, the current generation of  $^{68}\text{Ge}/^{68}\text{Ga}$  generators requires a dedicated radiopharmacy staff.

## Next generation SSTR PET ligands

**Table 3.** Comparison between the sensitivity of  $^{111}\text{In}$ -DTPA-octreotide planar and/or SPECT and  $^{68}\text{Ga}$ -DOTA-peptide PET as reported in several publications

Study	n	Gallium-68 peptide	Analysis level	Sensitivity $^{111}\text{In}$ -DTPA-octreotide	Sensitivity $^{68}\text{Ga}$ -DOTA-peptide	$\Delta$
Gabriel et al. [37]	84	-TOC	Patient	52%	97%	45%
Buchmann et al. [36]	27	-TOC	Region	65.1%	97.6%	32.5%
Van Binnebeek et al. [41]	53	-TOC	Lesion	60.1%	99.9%	39.8%
Morgat et al. [43]	19	-TOC	Lesion	20%	76%	56%
Srirajaskanthan et al. [44]	51	-TATE	Lesion	11.9%	74.3%	62.4%
Deppen et al. [38]	78	-TATE	Patient	72%	96%	24%
Sadowski et al. [40]	131	-TATE	Lesion	30.9%	95.1%	64.2%

(n = number of patients;  $\Delta$  = difference between the sensitivity of  $^{111}\text{In}$ -DTPA-octreotide and  $^{68}\text{Ga}$ -DOTA-peptide imaging).

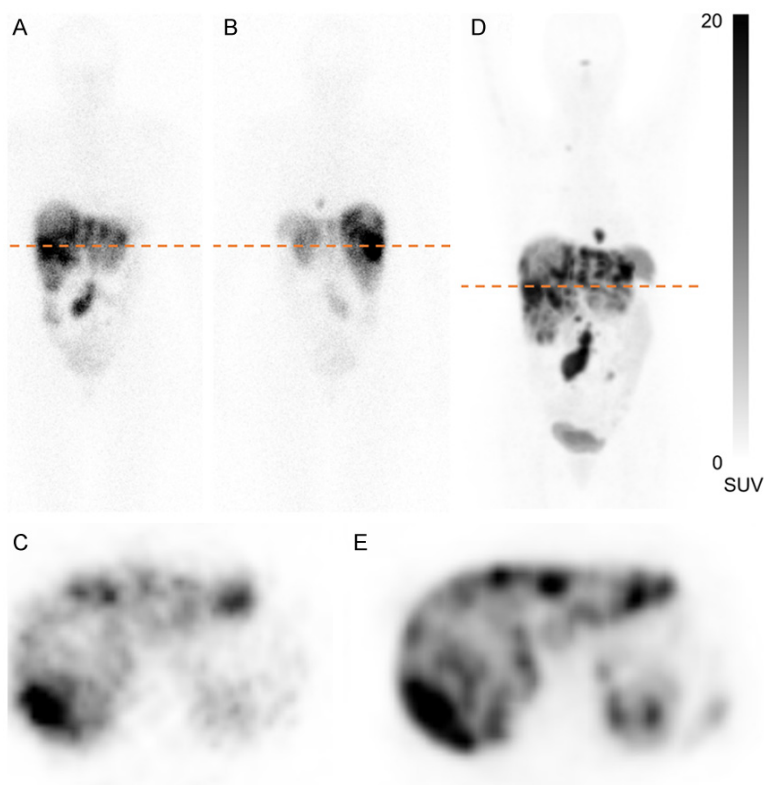


**Figure 3.** Head-to-head comparison of  $^{111}\text{In}$ -DTPA-octreotide scintigraphy (A: planar anterior, B: planar posterior, C: transversal SPECT image) and  $^{68}\text{Ga}$ -DOTATOC PET (D: maximal-intensity projection, E: transversal slice) of a patient with ileal NET and liver, lymph node and peritoneal metastases (patient data from: [41]). More lesions can be visualized on the  $^{68}\text{Ga}$ -DOTATOC PET images. Dashed lines in (A, B and D) denote the level of transversal slices in (C and E). Scale bar applies to PET images. (SUV = standardized uptake value).

Moreover, production and quality control of gallium-68 radiopharmaceuticals is subject to strict regulations imposed by pharmaceutical legislation [51, 52]. Nevertheless, due to the significant boost to clinical PET by the introduction of  $^{68}\text{Ga}$ -PSMA-HBED-CC [53], more and more nuclear medicine departments installed these  $^{68}\text{Ge}/^{68}\text{Ga}$  generators and production

facilities. Furthermore, the aforementioned issues may be largely solved with the next generation  $^{68}\text{Ge}/^{68}\text{Ga}$  generators that have received regulatory approval (e.g. IRE ELiT, Fleurus, Belgium) and the use of kit-based labeling approaches, such as SomaKit TOC™ (Advanced Accelerator Applications S.A.) and NE-TSPOT® (Advanced Accelerator Applications USA), that have received approval by the European Medicines Agency (EMA) and the Food and Drug Administration (FDA), respectively. As the overall activity yield per production batch is low (capacity of two to four patients per production) and half-life of gallium-68 is relatively short (68 minutes), there is only limited potential for centralized production and distribution. However, some possibilities may be opened up in this field by advances in the cyclotron production of gallium-68 [54].

Another disadvantage of gallium-68 is its relatively high positron energy ( $E_{\text{mean}} = 0.83$  MeV) and thus relatively long positron range ( $R_{\text{mean}} = 3.5$  mm), which may compromise spatial resolution [55]. Therefore, the possibilities of using other PET radionuclides for SSTR imaging are currently being explored. The physical characteristics of all radionuclides relevant for PET imaging discussed below are summarized in **Table 4**.

## Next generation SSTR PET ligands

**Table 4.** Physical characteristics relevant for PET imaging of the discussed radionuclides, with  $E_{\text{mean}}$  and  $E_{\text{max}}$  the mean and maximum positron energy, respectively, and  $R_{\text{mean}}$  and  $R_{\text{max}}$  the mean and maximum positron range calculated in water, respectively

Isotope	Half-life	Positron branching ratio (%)	$E_{\text{mean}}$ (MeV)	$E_{\text{max}}$ (MeV)	$R_{\text{mean}}$ (mm)	$R_{\text{max}}$ (mm)	Gamma branching ratio (%)	$E_{\gamma}$ (MeV)
Fluorine-18	109.8 min	96.9	0.250	0.634	0.6	2.4	-	-
Scandium-44	3.97 h	94.3	0.632	1.474	2.4	6.9	99.9	1.157
Copper-64	12.7 h	17.5	0.278	0.653	0.8	2.5	0.47	1.346
Gallium-68	67.8 min	87.7	0.836	1.899	3.5	9.2	3.2	1.077
		<i>1.2</i>	<i>0.353</i>	<i>0.822</i>	<i>1.1</i>	<i>3.4</i>		
		<b>88.9</b>	<b>0.829</b>		<b>3.5</b>			
Terbium-152	17.5 h	8.0	1.337	2.97	6.2	15.0	63.5	0.344
		<i>5.9</i>	<i>1.186</i>	<i>2.62</i>	<i>5.4</i>	<i>13.1</i>	9.5	0.271
		<b>20.3</b>	<b>1.14</b>		<b>5.1</b>			

For gallium-68 and terbium-152 only the positrons from the two highest positron branching ratios are listed in italics. The total positron branching ratio,  $E_{\text{mean}}$  and  $R_{\text{mean}}$  are listed in bold. Furthermore, the most relevant prompt gammas are given. Data from the Laboratoire National Henri Becquerel (<http://www.nucleide.org/Laraweb>), Brookhaven National Laboratory (<http://www.nndc.bnl.gov/nudat2>), and National Institute of Standards and Technology (<https://www.nist.gov/pml/radiation-dosimetry-data>).

### Copper-64

A frequently used non-standard PET radionuclide is copper-64 [54, 56]. Its half-life (12.7 hours) allows for centralized production, while its low positron energy ( $E_{\text{mean}} = 0.28$  MeV) corresponding to a short positron range ( $R_{\text{mean}} = 0.8$  mm) allows for high spatial resolution PET imaging [54, 55]. Copper-64 has a relatively low positron branching ratio of 17.5% and its decay is accompanied by emission of  $\beta^-$  particles and Auger electrons adding up to its radiation burden. Therefore, it could be used for therapeutic purposes as well, making it suited for theranostic applications [57], taking into account extensive shielding needed in practice due to the simultaneous high energy gamma and positron emission. Copper-64 can either be produced in a reactor or with a cyclotron [54, 57].

As early as 2001, Anderson *et al.* reported a first clinical evaluation of the dosimetry and pharmacokinetics of  $^{64}\text{Cu}$ -TETA-octreotide - copper-64 bound to octreotide through the chelator 1,4,8,11-tetraazacyclotetradecane-N,N',N'',N'''-tetraacetic acid (TETA) (see **Figure 1**) - in eight NET patients and its diagnostic properties were compared to  $^{111}\text{In}$ -DTPA-octreotide [58]. In two patients,  $^{64}\text{Cu}$ -TETA-octreotide detected clearly more lesions than  $^{111}\text{In}$ -DTPA-octreotide. In one patient mild uptake in a lung lesion was observed with  $^{111}\text{In}$ -DTPA-octreotide, but not picked up by  $^{64}\text{Cu}$ -TETA-octreotide.

However, delayed images which might have shown the lesion were not available for this patient. Pharmacokinetic assessment revealed fast blood clearance with partial urinary excretion. On the other hand, the percentage injected activity in the liver increased with time due to dissociation of the copper-64 isotope, indicating poor *in vivo* stability [57, 58].

The next clinical studies on copper-64 labeled SSAs date from more than 10 years later. Pfeifer *et al.* prospectively evaluated  $^{64}\text{Cu}$ -DOTATATE in a first-in-human study in 14 NET patients [59]. PET images with high spatial resolution were obtained. High and stable tumor-to-background ratios were observed on both the early (one hour post injection (p.i.)) and late (three hours p.i.) PET scans, indicating a high tracer internalization rate. Although some dissociation of copper-64 was suggested by increasing hepatic activity, *in vivo* stability of the tracer was sufficient for imaging purposes. All patients underwent conventional  $^{111}\text{In}$ -DTPA-octreotide SPECT/CT as well. Additional lesions were detected on  $^{64}\text{Cu}$ -DOTATATE PET in six patients (43%) and in five of these patients lesions were identified in organs not previously known as disease-involved. No lesions were observed with  $^{111}\text{In}$ -DTPA-octreotide SPECT that were not revealed by  $^{64}\text{Cu}$ -DOTATATE PET.

In a subsequent larger prospective study, Pfeifer *et al.* confirmed the diagnostic superiority of  $^{64}\text{Cu}$ -DOTATATE PET over  $^{111}\text{In}$ -DTPA-

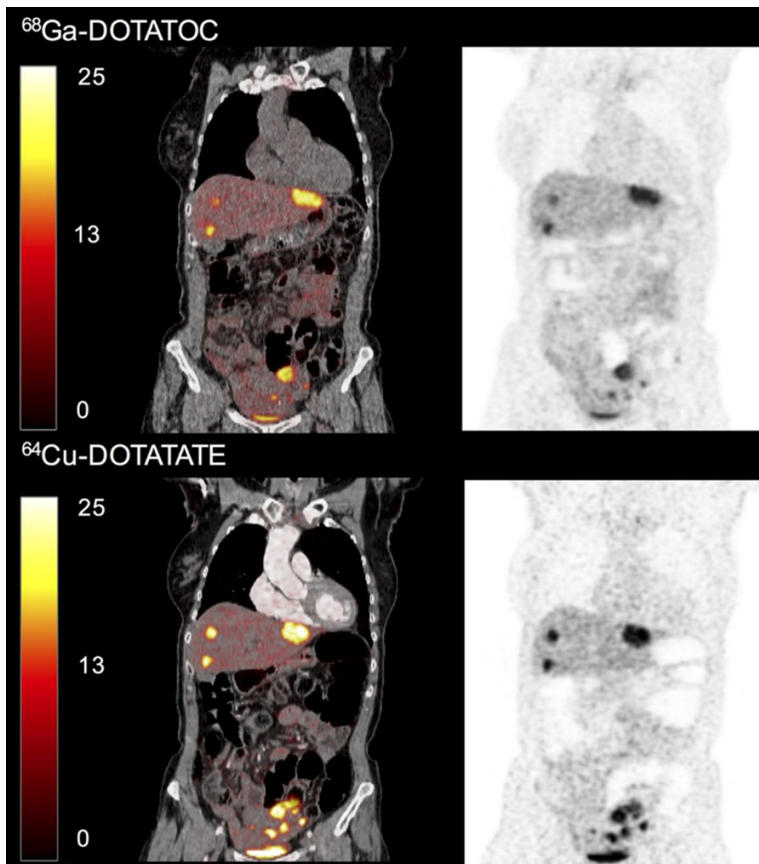


**Figure 4.** PET/CT (left) and PET (right) scans with  $^{68}\text{Ga}$ -DOTATOC and  $^{64}\text{Cu}$ -DOTATATE of a patient with intestinal NET and multiple metastases. Additional lesions are seen in the intestinal region with  $^{64}\text{Cu}$ -DOTATATE. This research was originally published in JNM. Johnbeck CB, Knigge U, Loft A, Berthelsen AK, Mortensen J, Oturai P, Langer SW, Elema DR and Kjaer A. Head-to-head comparison of  $^{64}\text{Cu}$ -DOTATATE and  $^{68}\text{Ga}$ -DOTATOC PET/CT: a prospective study of 59 patients with neuroendocrine tumors. J Nucl Med. 2017;58:451-457. © SNMMI.

octreotide SPECT by means of a head-to-head comparison in 112 NET patients [60]. PET images were acquired one hour after injection. The sensitivity and diagnostic accuracy of  $^{64}\text{Cu}$ -DOTATATE PET (both 97%) were significantly higher than those of conventional  $^{111}\text{In}$ -DTPA-octreotide SPECT (87% and 88%, respectively). Twice as many lesions were detected using  $^{64}\text{Cu}$ -DOTATATE PET, and more importantly, in 40 patients (36%) lesions were identified in organs not previously known as disease-involved. In 35 of these 40 patients the true-positive nature of these supplemental involved organs was confirmed by long-term follow-up of 42-60 months.

Of special interest is a recent study published by Johnbeck *et al.* comparing  $^{64}\text{Cu}$ -DOTATATE

and  $^{68}\text{Ga}$ -DOTATOC PET in 59 NET patients on a head-to-head basis [61]. On a patient level,  $^{64}\text{Cu}$ -DOTATATE and  $^{68}\text{Ga}$ -DOTATOC performed equally well. However,  $^{64}\text{Cu}$ -DOTATATE detected significantly more additional true-positive lesions, confirmed by at least 30 months of follow-up, than  $^{68}\text{Ga}$ -DOTATOC (33 versus 7). The authors attributed this difference in lesion detection rate to the shorter positron range of copper-64, with consequent higher spatial resolution and less partial volume effect, rather than to the use of a different peptide. **Figure 4** shows an example of a patient where more lesions are seen in the intestinal region with  $^{64}\text{Cu}$ -DOTATATE than with  $^{68}\text{Ga}$ -DOTATOC. Tumor-to-background ratios as a measure for image contrast were not significantly different between the two tracers. Although the radiation burden of  $^{64}\text{Cu}$ -DOTATATE is higher than that of  $^{68}\text{Ga}$ -DOTATOC (5.7-8.9 mSv vs. 2.8-4.6 mSv), the use of  $^{64}\text{Cu}$ -DOTATATE offers several advantages for use in routine clinical practices associated

to the half-life of copper-64, such as supply to peripheral sites from a central production unit and a more flexible scanning window ranging from one hour to at least three hours after injection. A preclinical evaluation of  $^{64}\text{Cu}$ -DOTATOC has been published [62], but to our knowledge no subsequent clinical studies have been performed.

Copper-64 has also been successfully coupled to TATE by means of a new bifunctional chelator, 5-(8-methyl3,6,10,13,16,19-hexaaza-bicyclo[6.6.6]icosan-1-ylamino)-5-oxopentanoic acid (MeCOSar), forming  $^{64}\text{Cu}$ -SARTATE [63]. Initial preclinical results are promising showing a high uptake in SSTR2-positive tumors [63]. Further preclinical and clinical studies on this new radiopharmaceutical are ongoing (Aus-

tralian New Zealand Clinical Trials Registry (ANZCTR) identifier: ACTRN12615000727549 [57].

### Fluorine-18

Among  $\beta^+$ -emitting radioisotopes, fluorine-18 is the most commonly used PET radionuclide in clinical practice and offers several logistic and physical advantages over gallium-68. Large amounts of fluorine-18 activity ( $> 370$  GBq) can be produced with a cyclotron and the half-life (109.8 minutes) is long enough to allow transport to remote hospitals without an on-site cyclotron and it is short enough to avoid extended irradiation of patients. Furthermore, it predominantly decays by positron emission (96.9%) with a low positron energy ( $E_{\text{mean}} = 0.25$  MeV) leading to a short positron range ( $R_{\text{mean}} = 0.6$  mm) [55].

Meisetschläger *et al.* evaluated the fluorine-18 labeled SSA, Gluc-Lys-( $^{18}\text{F}$ -fluoropropionyl)-Lys-Tyr<sup>3</sup>-octreotate (Gluc-Lys- $^{18}\text{F}$ FP-TOCA) (see **Figure 1**), in 25 patients with SSTR-positive tumors seen on  $^{111}\text{In}$ -DTPA-octreotide scan and performed a direct comparison in 16 of these patients [64]. Gluc-Lys- $^{18}\text{F}$ FP-TOCA showed a fast and high tumor uptake and was rapidly cleared from the blood, mainly through the kidneys. Tumor uptake reached a plateau at about 40 minutes after injection. In contrast to SSAs labeled with radiometals whose fragments remain trapped after cellular internalization, no such trapping has been observed for SSAs-based radiopharmaceuticals labeled with fluorine-18 such as Gluc-Lys- $^{18}\text{F}$ FP-TOCA [64, 65]. Nevertheless, more than twice as many lesions were observed with Gluc-Lys- $^{18}\text{F}$ FP-TOCA than with  $^{111}\text{In}$ -DTPA-octreotide. However, a serious impediment to the implementation of Gluc-Lys- $^{18}\text{F}$ FP-TOCA in routine clinical practice is its time-consuming multistep synthesis with limited radiochemical yield (20%-30%) [64]. Gluc-Lys- $^{18}\text{F}$ FP-TOCA has been applied in a few small clinical studies [65-67], but to our knowledge no further large clinical trials have been performed.

$^{18}\text{F}$ -fluoroethyl-triazole-Tyr<sup>3</sup>-octreotate ( $^{18}\text{F}$ -FET- $\beta$ AG-TOCA) (see **Figure 1**) represents an alternative  $^{18}\text{F}$ -octreotate radioligand with a more practical and shorter synthesis route and reasonable radiochemical yield [68]. Following the promising results in preclinical models [69],

Dubash *et al.* carried out a first-in-human study in nine NET patients evaluating the biodistribution and dosimetry of  $^{18}\text{F}$ -FET- $\beta$ AG-TOCA [70]. The tracer showed a rapid blood clearance with both renal and biliary elimination, whereas  $^{68}\text{Ga}$ -DOTA-peptides are mainly eliminated through the kidneys. As such, the highest absorbed dose was received by the gallbladder. Overall, the dosimetry of  $^{18}\text{F}$ -FET- $\beta$ AG-TOCA was similar to other fluorine-18 labeled tracers. Tumor-to-background ratios were high and comparable to values reported for  $^{68}\text{Ga}$ -DOTA-peptide PET, resulting in images with excellent contrast. Larger clinical trials for this promising tracer, including a direct comparison with  $^{68}\text{Ga}$ -DOTATATE PET/CT are currently ongoing [70].

Another fluorine-18 based SSA that is subject of recently initiated clinical trials in NET patients is  $\text{Al}^{18}\text{F}$ -1,4,7-triazacyclononane-1,4,7-triacetate-octreotide ( $\text{Al}^{18}\text{F}$ -NOTA-octreotide) (see **Figure 1**) (clinicaltrials.gov identifier: NCT03511768). The  $\text{Al}^{18}\text{F}$ -labeling method developed by McBride *et al.* combines the advantages of a chelator-based radiolabeling method with the unique properties of the radionuclide of choice, fluorine-18 [71]. In this method, fluorine is firmly bound to  $\text{Al}^{3+}$  forming  $^{18}\text{F}\text{AlF}$  which is then complexed by a suitable chelator, conjugated to a vector molecule of interest [72].  $\text{Al}^{18}\text{F}$ -NOTA-octreotide was developed by Laverman *et al.* and has been compared to  $^{111}\text{In}$ -DTPA-octreotide and  $^{68}\text{Ga}$ -NOTA-octreotide in preclinical models [73, 74].  $\text{Al}^{18}\text{F}$ -NOTA-octreotide proved to have the highest *in vitro* binding affinity for the SSTR (see **Table 2**), while a biodistribution in AR42J tumor-bearing mice showed that both tumor uptake and pharmacokinetics were similar with an excellent *in vitro* and *in vivo* stability.

Other promising fluorine-18 based tracers for SSTR imaging identified in preclinical studies include  $^{18}\text{F}$ -silicon-fluoride-acceptor (SiFA) and  $^{18}\text{F}$ -SiFA/*in* octreotate derivatives [75-77],  $^{18}\text{F}$ -trifluoroborate octreotate ( $^{18}\text{F}$ -AMBF<sub>3</sub>-TATE) [78] and  $^{18}\text{F}$ -fluoroglycosylated octreotate ( $^{18}\text{F}$ -FGlc-TATE) [79].

### Scandium-44

Scandium-44 has more recently emerged as a promising radionuclide for PET imaging. There are several methods to produce the radionu-

clide, for instance by means of a  $^{44}\text{Ti}/^{44}\text{Sc}$  generator, or using a cyclotron allowing to produce higher quantities [54, 80, 81]. Scandium-44 mainly decays through positron emission (94.3%) with a somewhat lower positron energy than gallium-68 ( $E_{\text{mean}} = 0.63$  MeV) and accordingly lower positron range ( $R_{\text{mean}} = 2.4$  mm). Its half-life of 3.97 hours is convenient for centralized production and distribution [81]. Even more promising is its use in theranostic applications. Although very similar to gallium(III)-68, the chemical behavior of scandium(III)-44 even more closely resembles that of the therapeutic radiometals, such as lutetium-177 and yttrium-90 [82]. Therefore, scandium-44 may represent an attractive alternative to gallium-68 for imaging and dosimetry prior to lutetium-177 based therapy [82]. However, the need for pre-therapy dosimetry has diminished due to the favorable results of the NETTER-1 trial. Moreover, since the half-life of scandium-44 is still limited compared to lutetium-177 (3.97 hours vs. 6.65 days) evaluation at time points later than three days is not possible. With the isotope scandium-47 (100%  $\beta^-$  emission), scandium-44 potentially also possesses a true therapeutic match, although research in this area is still in its infancy [83, 84].

Several preclinical studies have been published on various scandium labeled SSAs, such as  $^{44}\text{Sc}$ -DOTATOC [80, 85],  $^{\text{nat}}\text{Sc}$ -DOTATATE [86],  $^{44}\text{Sc}$ -DOTANOC [81, 87] and  $^{44}\text{Sc}$ -1,4,7-triazacyclononane, 1-glutaric acid-4,7-acetic acid (NODAGA)-NOC [87].

Rösch *et al.* performed a clinical proof-of-principle study using generator-produced  $^{44}\text{Sc}$ -DOTATOC [80, 88]. High quality PET images of a patient with SSTR-positive liver metastases were acquired at early time points and up to 18 hours after injection. Singh *et al.* published a proof-of-concept study using cyclotron-produced  $^{44}\text{Sc}$ -DOTATOC in two patients with metastatic NET [89]. Interestingly, scandium-44 was produced at the cyclotron facility at the Paul Scherrer Institut (PSI) in Switzerland and subsequently shipped over 600 km to Zentralklinik Bad Berka (ZBB) in Germany, requiring two and a half half-lives. Eight PET/CT scans were performed at various time points up to 23.5 hours after injection. Excellent tumor uptake was observed with increasing tumor-to-background values over the first four hours after injection.

Further clinical studies in larger patient cohorts are scheduled.

### *Terbium-152*

In light of theranostic applications, terbium gained the interest of researchers due to its four medically relevant radioisotopes: terbium-152 and terbium-155 for PET and SPECT imaging, respectively, and terbium-161 and terbium-149 for  $\beta^-$  and  $\alpha$ -therapy, respectively [84, 90]. The latter also offers the possibility of PET imaging, as demonstrated in a preclinical study evaluating  $^{149}\text{Tb}$ -DOTANOC in AR42J tumor-bearing mice [91]. Terbium-152, suited for diagnostic PET imaging, has a half-life of 17.5 hours and a positron branching ratio of 20.3% with a relatively high positron energy ( $E_{\text{mean}} = 1.14$  MeV) and thus higher positron range ( $R_{\text{mean}} = 5.1$ ) than gallium-68. Terbium-152 - as well as terbium-149 and -155 - can be produced by high-energy proton-induced spallation in tantalum foil targets [90]. Just like lutetium-177, it belongs to the group of radiolanthanides. Therefore, it can be stably coupled to the chelator DOTA and used for radiolabeling of SSAs [84]. In a preclinical study in AR42J tumor-bearing mice, the biodistribution of  $^{152}\text{Tb}$ -DOTANOC was found to be in good agreement with that of  $^{177}\text{Lu}$ -DOTANOC [92]. These findings suggest that terbium-152 could serve as a theranostic agent for lutetium-177 based therapy. A clinical proof-of-concept was published by Baum *et al.* in 2017 using  $^{152}\text{Tb}$ -DOTATOC in a patient with well-differentiated metastatic NET of the terminal ileum [93]. Terbium-152 was produced at the Isotope mass Separator On-Line (ISOLDE) facility in CERN in Switzerland, shipped to PSI for separation from the collection matrix and quality control and finally transported to ZBB in Germany for radiolabeling. PET/CT images were acquired at various time points up to 24 hours after injection. All known tumor lesions, visualized on a previous  $^{68}\text{Ga}$ -DOTATOC PET scan, were clearly identified. Images were noisier, compared to this previous gallium-68 based PET. This was attributed to the lack of prompt  $\gamma$ -correction by the PET software. Even at 24 hours after injection, increased uptake was observed in several metastases. The authors concluded that the longer half-life of terbium-152, as compared to gallium-68, enabling imaging at later time-points, makes terbium-152 particularly valuable for dosime-

try prior to radionuclide therapy [93]. However, the production of terbium-152 is challenging and currently imposes an important constraint on its implementation in routine clinical practice.

### Vector

Developments in SSTR PET radiopharmaceuticals do not only focus on the choice of radionuclide but also on the characteristics of the vector molecule. The radiopharmaceuticals described above contain the somatostatin receptor agonist octreotide, or an analog of octreotide, as vector molecule, with a predominance of TOC and TATE. Improved tumor targeting may be achieved for instance by using vector molecules having a higher binding affinity for the SSTR or a broader affinity profile for the different receptor subtypes or by using compounds recognizing a higher number of binding sites, such as the SSTR antagonists.

### Somatostatin receptor agonists

Many tumor types that show SSTR expression, predominantly express SSTR2 [12], which makes it the main target for the development of SSTR ligands for imaging and therapy. However, as mentioned above, a wide variability in subtype expression has been observed across and within different tumor types [12]. Therefore, there is great interest in SSTR ligands with a broader affinity profile to increase tumor uptake and to expand the number of tumors eligible for SSTR imaging [94]. Of the  $^{68}\text{Ga}$ -DOTA-peptides currently used in clinical practice,  $^{68}\text{Ga}$ -DOTANOC has the widest affinity profile with high affinities for SSTR2, SSTR5 and to a lesser extent SSTR3 [23]. However, as discussed above, there is no conclusive evidence to prefer this ligand in clinical practice and large trials are warranted [49], but properly powered prospective trials testing this hypothesis will probably not be available for a long time. Another SSA that has been evaluated early on in clinical trials is the long-acting SSA lanreotide (see **Figure 1**). Coupled to the chelator DOTA, DOTA-lanreotide (DOTALAN) and the radiolabeled compounds  $^{111}\text{In}/^{90}\text{Y}$ -DOTALAN showed a high affinity for SSTR subtype 2-5 [95]. However, this was only confirmed for SSTR2 and 5 by Reubi *et al.* [23]. Following promising clinical results with  $^{111}\text{In}$ -DOTALAN [96, 97], DOTALAN was labeled with gallium-68

to allow PET imaging. After an initial positive evaluation of  $^{68}\text{Ga}$ -DOTALAN in 11 patients with lung cancer (three small cell and three non-small cell lung cancer) or thyroid cancer (two medullary and three radioiodine negative thyroid cancer) [98], the tracer was used to identify patients who might benefit from PRRT with  $^{90}\text{Y}$ -DOTALAN in a group of NET patients not qualified for PRRT with  $^{68}\text{Ga}$ -DOTATOC despite progressive disease [99]. Tumor-to-background ratios were significantly higher for  $^{68}\text{Ga}$ -DOTATOC and more tumor sites (106 vs. 53) were detected with  $^{68}\text{Ga}$ -DOTATOC than with  $^{68}\text{Ga}$ -DOTALAN. Demirci *et al.* compared  $^{68}\text{Ga}$ -DOTALAN with  $^{68}\text{Ga}$ -DOTATATE in a group of 11 NET patients and one patient with meningioma.  $^{68}\text{Ga}$ -DOTATATE performed better than  $^{68}\text{Ga}$ -DOTALAN with a significantly higher lesion uptake and higher lesion detection rate (63 vs. 23 out of a total of 67 tumor lesions detected with both tracers) [100]. Traub-Weidinger *et al.* evaluated the SSTR status in a heterogeneous group of thyroid cancer patients with progressive disease using two tracers with a distinct SSTR subtype affinity profile,  $^{68}\text{Ga}$ -DOTALAN and  $^{68}\text{Ga}$ -DOTATOC, in 28 patients [101]. On a patient basis, 12 patients were negative with both SSTR tracers, while mixed results were observed in three patients (two patients negative with  $^{68}\text{Ga}$ -DOTALAN, but positive with  $^{68}\text{Ga}$ -DOTATOC and one patient vice versa). On a region-based analysis half of the 38 regions positive on SSTR imaging (out of a total of 196 regions) showed mixed results. The authors concluded that, due to the heterogeneous SSTR profile of thyroid cancer lesions, patients with progressive disease may benefit from imaging with different SSTR PET tracers for individualized targeted therapy stratification.

In a first attempt to develop an actual pansomatostatin radiopharmaceutical with high affinity for all SSTR subtypes, the cyclooctapeptide KE108 with pansomatostatin characteristics was modified to couple the chelator DOTA (DOTA-D-Dab-Arg-Phe-Phe-D-Trp-Lys-Thr-Phe or KE88) and allow subsequent radiolabeling with indium-111 and gallium-68 [102]. Although the resulting tracers were able to bind all SSTR subtypes with high affinity, *in vitro* internalization of the ligand-receptor complex for the SSTR2 was low compared to the SSTR3 and this was reflected by a low *in vivo* uptake observed in SSTR2-expressing tumors and fast

wash out [102]. In another preclinical study, Fani *et al.* synthesized and evaluated several bicyclic somatostatin-based analogs of which DOTA-Tyr-cyclo(DAB-Arg-cyclo(Cys-Phe-D-Trp-Lys-Thr-Cys)) or AM3, showing a high affinity for SSTR2, SSTR3 and SSTR5, was the most promising [103]. Efficient background clearance and high tumor uptake with  $^{68}\text{Ga}$ -AM3 were observed in SSTR2 tumor-bearing mice. Tatsi *et al.* used the native peptide hormone somatostatin-14 (SS14) as a basis to develop two SS14-derived analogs with a high affinity for all SSTR subtypes and label them with indium-111 [104]. However, both tracers showed poor *in vivo* stability. Similarly, Maina *et al.* used the more stable native peptide somatostatin-28 (SS28) as a basis for the development of DOTA-Ser,Leu,D-Trp,Tyr-SS28 (DOTA-LTT-SS28) and the radioligand  $^{111}\text{In}$ -DOTA-LTT-SS28 [105]. The compounds displayed a high affinity for all SSTR subtypes and triggered internalization of SSTR2, SSTR3 and SSTR5.  $^{111}\text{In}$ -DOTA-LTT-SS28 showed a high and specific uptake in SSTR2-, SSTR3- and SSTR5-expressing xenografts in mice and a much higher *in vivo* stability than the SS14-derived tracers developed by Tatsi *et al.* The authors concluded that  $^{111}\text{In}$ -DOTA-LTT-SS28 is the first true (pan)somatostatin radioligand and may serve as a model for the further development of pansomatostatin radioligands [105]. Very recently, Liu *et al.* reported the development of gallium-68 labeled pasireotide (SOM230 or PA1), a long-acting synthetic SSA with a high affinity for SSTR1, SSTR2, SSTR3 and SSTR5 [106, 107]. The resulting radiotracer  $^{68}\text{Ga}$ -DOTA-PA1 displayed a significantly higher *in vitro* uptake than  $^{68}\text{Ga}$ -DOTATATE in three human lung cancer cell lines: lung adenocarcinoma (A549), lung squamous carcinoma (H520) and pulmonary giant cell carcinoma (PG). PET images of A549 tumor-bearing mice showed a high tumor uptake and better signal-to-noise ratio with  $^{68}\text{Ga}$ -DOTA-PA1 than with  $^{68}\text{Ga}$ -DOTATATE and the PET signal correlated with the total expression of SSTRs and not only SSTR2, as determined by Western blotting. The authors concluded that  $^{68}\text{Ga}$ -DOTA-PA1 and its analogs may hold potential for SSTR imaging in clinical practice, especially lung tumors [107].

Therapeutic purposes have also driven some new developments in the vector part of SSTR ligands aiming for higher tumor retention to

improve therapeutic efficiency and preferably lower kidney dose to reduce PRRT toxicity. A recent example is given by Tian *et al.* who conjugated an Evans blue (EB) analog onto octreotate which allows reversible binding of EB-TATE to albumin to prolong half-life in blood, resulting in a SSA with long circulation time [108]. EB-TATE was then labeled with yttrium-90 through the chelator DOTA and injected in AR42J tumor bearing mice.  $^{90}\text{Y}$ -DOTA-EB-TATE showed high tumor uptake resulting in a complete regression of the tumors [108]. These promising results were quickly translated into a first-in-human clinical trial by Zhang *et al.* evaluating the safety, pharmacokinetics and dosimetry of  $^{177}\text{Lu}$ -DOTA-EB-TATE in five NET patients as compared to  $^{177}\text{Lu}$ -DOTATATE in three other NET patients [109]. The new compound was well tolerated without adverse symptoms. Tumor dose was 7.9-fold higher with  $^{177}\text{Lu}$ -DOTA-EB-TATE, while the effective dose was not significantly different between  $^{177}\text{Lu}$ -DOTA-EB-TATE and  $^{177}\text{Lu}$ -DOTATATE. However, kidney and bone marrow dose increased 3.2- and 18.2-fold, respectively [109], so this radiopharmaceutical does not offer an improved therapeutic ratio compared to the current radiopharmaceutical of choice,  $^{177}\text{Lu}$ -DOTATATE.

### Somatostatin receptor antagonists

All SSTR-targeting radiopharmaceuticals described above are somatostatin agonists. After binding to the SSTR, the ligand-receptor complex is usually internalized, allowing tracer metabolites to accumulate in the target cells [110]. For a long time, it was believed that this process of internalization and subsequent accumulation of the radioligands was essential for high-contrast imaging of SSTR-positive lesions [111]. However, in 2006, Ginj *et al.* observed in cell cultures expressing human SSTR2 and SSTR3, that antagonists labeled considerably more receptor sites than agonists [110]. This was reflected by the significantly higher tumor uptake seen in mice bearing SSTR2 and SSTR3-expressing tumors after injection with the corresponding antagonist as compared to those injected with the agonist [110]. Especially striking was the fact that counterintuitive to this observation the SSTR2 antagonist,  $^{111}\text{In}$ -DOTA-pNO<sub>2</sub>-Phe-c(D-Cys-Tyr-D-Trp-Lys-Thr-Cys)D-TyrNH<sub>2</sub> ( $^{111}\text{In}$ -DOTA-BASS)

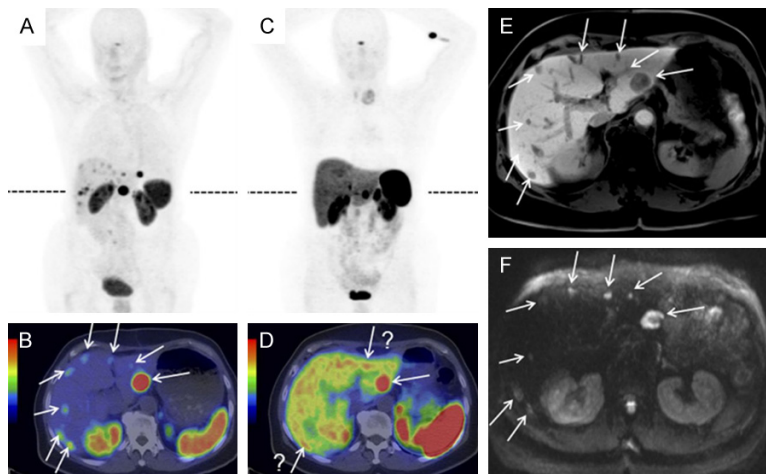


**Figure 5.** Maximal-intensity projections (A and C) and PET/CT (B and D) scans with  $^{68}\text{Ga}$ -NODAGA-JR11 (A and B) and  $^{68}\text{Ga}$ -DOTATOC of a patient with ileal NET and bilobar liver metastases. Liver magnetic resonance imaging (MRI) was performed four months later, with delayed post-contrast acquisitions (E) and diffusion-weighted images (F), confirming the additional metastases missed or questionable (arrow with question mark) with  $^{68}\text{Ga}$ -DOTATOC. Note the lower background activity in the liver, intestine and thyroid with  $^{68}\text{Ga}$ -NODAGA-JR11. Dashed lines in (A and C) denote the level of transverse slices in (B, D, E and F). This research was originally published in JNM. Nicolas GP, Schreiter N, Kaul F, Uiters J, Bouterfa H, Kaufmann J, Erlanger TE, Cathomas R, Christ E, Fani M and Wild D. Sensitivity comparison of  $^{68}\text{Ga}$ -OPS202 and  $^{68}\text{Ga}$ -DOTATOC PET/CT in patients with gastroenteropancreatic neuroendocrine tumors: a prospective phase II imaging study. *J Nucl Med.* 2018;59:915-921. © SNMMI.

(see **Figure 1**), showed a more than sevenfold lower affinity for the SSTR2 than the SSTR2 agonist  $^{111}\text{In}$ -DTPA-TATE in this study (50% inhibitory concentration ( $\text{IC}_{50}$ ) of  $9.4 \pm 0.4$  nM vs.  $1.3 \pm 0.2$  nM) [110]. In 2011, Wild *et al.* published a pilot study in five patients, one metastatic follicular thyroid carcinoma and four NETs, evaluating the biodistribution, tumor uptake and detection of tumor lesions with the SSTR antagonist  $^{111}\text{In}$ -DOTA-BASS in a head-to-head comparison with  $^{111}\text{In}$ -DTPA-octreotide [112]. Tumor uptake was up to four times higher with the antagonist, while renal, liver and spleen uptake were lower.  $^{111}\text{In}$ -DOTA-BASS detected more lesions than  $^{111}\text{In}$ -DTPA-octreotide (25 vs. 17 out of 28). The three missed bone lesions were negative on the  $^{111}\text{In}$ -DTPA-octreotide scan as well.

Further advances in the preclinical setting in search of more potent SSTR2 antagonists labeled with PET radioisotopes led to the identification of Cpa-c[D-Cys-Aph(Hor)D-Aph(Cbm)-Lys-Thr-Cys]-D-Tyr-NH<sub>2</sub> (JR11) (see **Figure 1**) as a promising compound for implementation in the clinical field [113]. Based on the results of

previous affinity studies and an *in vivo* biodistribution study [114],  $^{68}\text{Ga}$ -NODAGA-JR11 ( $^{68}\text{Ga}$ -OPS202) was selected for a first clinical evaluation by Nicolas *et al.* [115, 116]. 12 patients with GEP NET and a positive  $^{68}\text{Ga}$ -DOTATOC PET/CT scan in the previous six months were administered two microdoses of  $^{68}\text{Ga}$ -NODAGA-JR11 with ascending peptide masses at different study visits and underwent subsequent PET/CT scans.  $^{68}\text{Ga}$ -NODAGA-JR11 showed a fast blood clearance and favorable biodistribution with both peptide doses as compared to  $^{68}\text{Ga}$ -DOTATOC (lower hepatic, pancreatic, gastro-intestinal and splenic uptake with  $^{68}\text{Ga}$ -NODAGA-JR11) [115, 116]. This was reflected by higher tumor-to-background ratios observed with  $^{68}\text{Ga}$ -NODAGA-JR11 and further translates to a significantly higher number

of detected tumor lesions and higher lesion-based overall sensitivity (94% and 88% for 50  $\mu\text{g}$  and 15  $\mu\text{g}$   $^{68}\text{Ga}$ -NODAGA-JR11, respectively, vs. 59% for  $^{68}\text{Ga}$ -DOTATOC) [116]. An example is shown in **Figure 5**. The effective dose is in line with  $^{68}\text{Ga}$ -DOTA-peptides ( $24 \pm 2$   $\mu\text{Sv}/\text{MBq}$  for  $^{68}\text{Ga}$ -NODAGA-JR11 vs.  $21 \pm 3$   $\mu\text{Sv}/\text{MBq}$  for  $^{68}\text{Ga}$ -DOTATATE and  $^{68}\text{Ga}$ -DOTATOC [117]), although some differences in organ doses are observed due to a slightly different biodistribution [115]. Overall,  $^{68}\text{Ga}$ -NODAGA-JR11 was well tolerated [115]. However, SSTR antagonists could possibly counteract the effects of SSAs, which may be important in patients with functioning NETs [111]. Therefore, caution is required in anticipation of more safety data [111]. Currently a multicenter clinical trial evaluating the optimal dose and safety of  $^{68}\text{Ga}$ -NODAGA-JR11 for PET imaging is ongoing (clinicaltrials.gov identifier: NCT03220217).

The higher tumor uptake achieved with SSTR antagonists may also prove useful for therapeutic purposes. Preclinical studies comparing  $^{177}\text{Lu}$ -DOTA-JR11 ( $^{177}\text{Lu}$ -OPS201) with  $^{177}\text{Lu}$ -DOTATATE observed higher tumor uptake and lon-

ger residence times, resulting in higher tumor doses delivered by the antagonist as compared to the agonist [118, 119]. In a clinical pilot study by Wild *et al.* in four patients with progressive NETs, more than threefold higher tumor doses and twofold higher tumor-to-kidney and tumor-to-bone marrow dose ratios were observed using a test dose of  $^{177}\text{Lu}$ -DOTA-JR11 as compared to  $^{177}\text{Lu}$ -DOTATATE [120]. All patients were subsequently treated with  $^{177}\text{Lu}$ -DOTA-JR11, resulting in partial remission in two patients, mixed response in one patient and stable disease in the last patient, and as such proving the clinical feasibility of PRRT using radiolabeled SSTR antagonists. Currently, a multicenter clinical trial evaluating the safety and efficacy of  $^{177}\text{Lu}$ -DOTA-JR11 (clinicaltrials.gov identifier: NCT02592707) as well as a study evaluating the theranostic couple  $^{68}\text{Ga}$ -DOTA-JR11 and  $^{177}\text{Lu}$ -DOTA-JR11 (clinicaltrials.gov identifier: NCT02609737) are ongoing.

Radiolabeled SSTR antagonists might also prove to be especially useful for imaging and therapy of cancer types with a typically lower SSTR expression such as breast cancer [121]. Several preclinical studies observed enhanced tumor targeting in various human SSTR2-expressing tumor samples, including breast carcinoma, by means of *in vitro* autoradiography using an SSTR2 antagonist in comparison to the SSTR2 agonist [121-123]. This finding was not confirmed in a recent preclinical study by Dude *et al.* using the human luminal breast cancer model, ZR-75-1, with endogenous SSTR2 expression and negligible expression of other SSTR subtypes, where  $^{68}\text{Ga}$ -NODAGA-JR11 had a lower tumor uptake than  $^{68}\text{Ga}$ -DOTATOC and  $^{68}\text{Ga}$ -DOTATATE [124]. This was tentatively explained by the authors by the fact that they used an endogenously expressing cell line, which may have a lower amount of low-affinity, antagonist-specific binding sites. Interestingly, although  $^{68}\text{Ga}$ -DOTATATE has a higher affinity for the SSTR2 than  $^{68}\text{Ga}$ -DOTATOC, the latter was found to have the highest tumor uptake. Additional studies are warranted to further investigate the role of SSTR2 antagonists in breast cancer imaging [124].

### Conclusion

Advances in SSTR PET ligands occur on two major fronts: the radionuclide and the peptide vector. Other radionuclides could offer a solu-

tion to practical, economical and regulatory barriers to the adoption of  $^{68}\text{Ga}$ -DOTA-peptide PET, with additional physical advantages such as lower positron range and longer half-life. Developments concerning peptide vectors are mainly driven by the need for improved lesion targeting, especially for tumors with low SSTR expression. Therefore, advances on both fronts are largely complementary. Several promising new PET ligands for clinical SSTR imaging are currently in the pipeline and good results have been demonstrated in phase II trials. Clinical adoption in the near future is a realistic scenario.

### Acknowledgements

This research was funded by the project from “Kom op tegen Kanker”: “PET/MR imaging of the norepinephrine transporter and somatostatin receptor in neural crest and neuroendocrine tumors for better radionuclide therapy selection” and received support from Research Foundation-Flanders (FWO) (GOD88-17N). Frederik Cleeren is a Postdoctoral Fellow of FWO (12R3119N). Christophe M. Deroose is a Senior Clinical Investigator at the FWO.

### Disclosure of conflict of interest

Christophe M. Deroose received grants and personal fees from Novartis, Terumo, AAA, Ipsen, Sirtex, Bayer outside the submitted work.

**Address correspondence to:** Christophe M Deroose, Nuclear Medicine, University Hospitals Leuven, UZ Leuven, Campus Gasthuisberg, Nucleaire Geneeskunde, Herestraat 49, BE-3000 Leuven, Belgium. Tel: +32 16 34 37 15; Fax: +32 16 34 37 59; E-mail: christophe.deroose@uzleuven.be

### References

- [1] Schonbrunn A and Tashjian H Jr. Characterization of functional receptors for somatostatin in rat pituitary cells in culture. *J Biol Chem* 1978; 253: 6473-6483.
- [2] Hoyer D, Bell GI, Berelowitz M, Epelbaum J, Feniuk W, Humphrey PP, O'Carroll AM, Patel YC, Schonbrunn A, Taylor JE, et al. Classification and nomenclature of somatostatin receptors. *Trends Pharmacol Sci* 1995; 16: 86-88.
- [3] Patel YC. Somatostatin and its receptor family. *Front Neuroendocrinol* 1999; 20: 157-198.
- [4] Weckbecker G, Lewis I, Albert R, Schmid HA, Hoyer D and Bruns C. Opportunities in somatostatin research: biological, chemical and

## Next generation SSTR PET ligands

- therapeutic aspects. *Nat Rev Drug Discovery* 2003; 2: 999-1017.
- [5] Reubi JC, Kvols L, Krenning E and Lamberts SW. Distribution of somatostatin receptors in normal and tumor tissue. *Metabolism* 1990; 39: 78-81.
- [6] Patel YC, Greenwood MT, Panetta R, Demchyshyn L, Niznik H and Srikant CB. The somatostatin receptor family. *Life Sci* 1995; 57: 1249-1265.
- [7] Reubi JC, Schaer JC, Markwalder R, Waser B, Horisberger U and Laissue J. Distribution of somatostatin receptors in normal and neoplastic human tissues: recent advances and potential relevance. *Yale J Biol Med* 1997; 70: 471-479.
- [8] Volante M, Bozzalla-Cassione F and Papotti M. Somatostatin receptors and their interest in diagnostic pathology. *Endocr Pathol* 2004; 15: 275-291.
- [9] Reubi JC, Laissue J, Krenning E and Lamberts SW. Somatostatin receptors in human cancer: incidence, characteristics, functional correlates and clinical implications. *J Steroid Biochem Mol Biol* 1992; 43: 27-35.
- [10] Reubi JC. Somatostatin and other peptide receptors as tools for tumor diagnosis and treatment. *Neuroendocrinology* 2004; 80 Suppl 1: 51-56.
- [11] Volante M, Rosas R, Allia E, Granata R, Baragli A, Muccioli G and Papotti M. Somatostatin, cortistatin and their receptors in tumours. *Mol Cell Endocrinol* 2008; 286: 219-229.
- [12] Reubi JC, Waser B, Schaer JC and Laissue JA. Somatostatin receptor sst1-sst5 expression in normal and neoplastic human tissues using receptor autoradiography with subtype-selective ligands. *Eur J Nucl Med* 2001; 28: 836-846.
- [13] Eriksson B and Oberg K. Summing up 15 years of somatostatin analog therapy in neuroendocrine tumors: future outlook. *Ann Oncol* 1999; 10 Suppl 2: S31-38.
- [14] Pavel M, Valle JW, Eriksson B, Rinke A, Caplin M, Chen J, Costa F, Falkerby J, Fazio N, Gorbounova V, de Herder W, Kulke M, Lombard-Bohas C, O'Connor J, Sorbye H and Garcia-Carbonero R. ENETS consensus guidelines for the standards of care in neuroendocrine neoplasms: systemic therapy-biotherapy and novel targeted agents. *Neuroendocrinology* 2017; 105: 266-280.
- [15] Deroose CM, Hindie E, Kebebew E, Goichot B, Pacak K, Taieb D and Imperiale A. Molecular imaging of gastroenteropancreatic neuroendocrine tumors: current status and future directions. *J Nucl Med* 2016; 57: 1949-1956.
- [16] Barrio M, Czernin J, Fanti S, Ambrosini V, Binse I, Du L, Eiber M, Herrmann K and Fendler WP. The impact of somatostatin receptor-directed PET/CT on the management of patients with neuroendocrine tumor: a systematic review and meta-analysis. *J Nucl Med* 2017; 58: 756-761.
- [17] Sundin A, Arnold R, Baudin E, Cwikla JB, Eriksson B, Fanti S, Fazio N, Giammarile F, Hicks RJ, Kjaer A, Krenning E, Kwekkeboom D, Lombard-Bohas C, O'Connor JM, O'Toole D, Rockall A, Wiedenmann B, Valle JW and Vullierme MP. ENETS consensus guidelines for the standards of care in neuroendocrine tumors: radiological, nuclear medicine & hybrid imaging. *Neuroendocrinology* 2017; 105: 212-244.
- [18] Hicks RJ, Kwekkeboom DJ, Krenning E, Bodei L, Grozinsky-Glasberg S, Arnold R, Borbath I, Cwikla J, Toumpanakis C, Kaltsas G, Davies P, Horsch D, Tiensuu Janson E and Ramage J. ENETS consensus guidelines for the standards of care in neuroendocrine neoplasia: peptide receptor radionuclide therapy with radiolabeled somatostatin analogues. *Neuroendocrinology* 2017; 105: 295-309.
- [19] Strosberg J, El-Haddad G, Wolin E, Hendifar A, Yao J, Chasen B, Mittra E, Kunz PL, Kulke MH, Jacene H, Bushnell D, O'Dorisio TM, Baum RP, Kulkarni HR, Caplin M, Lebtahi R, Hobday T, Delpassand E, Van Cutsem E, Benson A, Srirajkanthan R, Pavel M, Mora J, Berlin J, Grande E, Reed N, Seregini E, Oberg K, Lopera Sierra M, Santoro P, Thevenet T, Erion JL, Ruszniewski P, Kwekkeboom D and Krenning E. Phase 3 trial of <sup>177</sup>Lu-dotatate for midgut neuroendocrine tumors. *N Engl J Med* 2017; 376: 125-135.
- [20] Sugiura G, Kuhn H, Sauter M, Haberkorn U and Mier W. Radiolabeling strategies for tumor-targeting proteinaceous drugs. *Molecules* 2014; 19: 2135-2165.
- [21] Nedrow JR, White AG, Modi J, Nguyen K, Chang AJ and Anderson CJ. Positron emission tomographic imaging of copper 64- and gallium 68-labeled chelator conjugates of the somatostatin agonist tyr3-octreotate. *Mol Imaging* 2014; 13: 1-13.
- [22] Johnbeck CB, Knigge U and Kjaer A. PET tracers for somatostatin receptor imaging of neuroendocrine tumors: current status and review of the literature. *Future Oncol* 2014; 10: 2259-2277.
- [23] Reubi JC, Schar JC, Waser B, Wenger S, Hoppeler A, Schmitt JS and Macke HR. Affinity profiles for human somatostatin receptor subtypes SST1-SST5 of somatostatin radiotracers selected for scintigraphic and radiotherapeutic use. *Eur J Nucl Med* 2000; 27: 273-282.
- [24] Krenning EP, Bakker WH, Breeman WA, Koper JW, Kooij PP, Ausema L, Lameris JS, Reubi JC and Lamberts SW. Localisation of endocrine-related tumours with radioiodinated analogue of somatostatin. *Lancet* 1989; 1: 242-244.

## Next generation SSTR PET ligands

- [25] Krenning EP, Bakker WH, Kooij PP, Breeman WA, Oei HY, de Jong M, Reubi JC, Visser TJ, Bruns C, Kwekkeboom DJ, et al. Somatostatin receptor scintigraphy with indium-111-DTPA-D-Phe-1-octreotide in man: metabolism, dosimetry and comparison with iodine-123-Tyr-3-octreotide. *J Nucl Med* 1992; 33: 652-658.
- [26] Krenning EP, Kwekkeboom DJ, Bakker WH, Breeman WA, Kooij PP, Oei HY, van Hagen M, Postema PT, de Jong M, Reubi JC, et al. Somatostatin receptor scintigraphy with [<sup>111</sup>In-DTPA-D-Phe1]- and [123I-Tyr3]-octreotide: the Rotterdam experience with more than 1000 patients. *Eur J Nucl Med* 1993; 20: 716-731.
- [27] Ambrosini V, Fani M, Fanti S, Forrer F and Maecke HR. Radiopeptide imaging and therapy in Europe. *J Nucl Med* 2011; 52 Suppl 2: 42S-55S.
- [28] Gabriel M, Decristoforo C, Donnemiller E, Ulmer H, Watfah Rychlinski C, Mather SJ and Moncayo R. An inpatient comparison of <sup>99m</sup>Tc-EDDA/HYNIC-TOC with <sup>111</sup>In-DTPA-octreotide for diagnosis of somatostatin receptor-expressing tumors. *J Nucl Med* 2003; 44: 708-716.
- [29] Mikolajczak R and Maecke HR. Radiopharmaceuticals for somatostatin receptor imaging. *Nucl Med Rev Cent East Eur* 2016; 19: 126-132.
- [30] Heppeler A, Froidevaux S, Macke HR, Jermann E, Behe M, Powell P and Hennig M. Radiometal-labelled macrocyclic chelator-derivatised somatostatin analogue with superb tumour-targeting properties and potential for receptor-mediated internal radiotherapy. *Chem-Eur J* 1999; 5: 1974-1981.
- [31] Al-Nahas A, Win Z, Szyszko T, Singh A, Nanni C, Fanti S and Rubello D. Gallium-68 PET: a new frontier in receptor cancer imaging. *Anti-cancer Res* 2007; 27: 4087-4094.
- [32] Henze M, Schuhmacher J, Hipp P, Kowalski J, Becker DW, Doll J, Macke HR, Hofmann M, Debus J and Haberkorn U. PET imaging of somatostatin receptors using [68Ga]DOTA-D-Phe1-Tyr3-octreotide: first results in patients with meningiomas. *J Nucl Med* 2001; 42: 1053-1056.
- [33] Hofmann M, Maecke H, Borner R, Weckesser E, Schoffski P, Oei L, Schumacher J, Henze M, Heppeler A, Meyer J and Knapp H. Biokinetics and imaging with the somatostatin receptor PET radioligand (68Ga)-DOTATOC: preliminary data. *Eur J Nucl Med* 2001; 28: 1751-1757.
- [34] Hope TA, Bergsland EK, Bozkurt MF, Graham M, Heaney AP, Herrmann K, Howe JR, Kulke MH, Kunz PL, Mailman J, May L, Metz DC, Millo C, O'Dorisio S, Reidy-Lagunes DL, Soulen MC and Strosberg JR. Appropriate use criteria for somatostatin receptor PET imaging in neuroendocrine tumors. *J Nucl Med* 2018; 59: 66-74.
- [35] Wild D, Macke HR, Waser B, Reubi JC, Ginj M, Rasch H, Muller-Brand J and Hofmann M. <sup>68</sup>Ga-DOTANOC: a first compound for PET imaging with high affinity for somatostatin receptor subtypes 2 and 5. *Eur J Nucl Med Mol Imaging* 2005; 32: 724.
- [36] Buchmann I, Henze M, Engelbrecht S, Eisenhut M, Runz A, Schafer M, Schilling T, Haufe S, Herrmann T and Haberkorn U. Comparison of <sup>68</sup>Ga-DOTATOC PET and <sup>111</sup>In-DTPAOC (Octreoscan) SPECT in patients with neuroendocrine tumours. *Eur J Nucl Med Mol Imaging* 2007; 34: 1617-1626.
- [37] Gabriel M, Decristoforo C, Kendler D, Dobrozemsky G, Heute D, Uprimny C, Kovacs P, Von Guggenberg E, Bale R and Virgolini JJ. <sup>68</sup>Ga-DOTA-Tyr<sup>3</sup>-octreotide PET in neuroendocrine tumors: comparison with somatostatin receptor scintigraphy and CT. *J Nucl Med* 2007; 48: 508-518.
- [38] Deppen SA, Liu E, Blume JD, Clanton J, Shi C, Jones-Jackson LB, Lakhani V, Baum RP, Berlin J, Smith GT, Graham M, Sandler MP, Delbeke D and Walker RC. Safety and efficacy of <sup>68</sup>Ga-DOTATATE PET/CT for diagnosis, staging, and treatment management of neuroendocrine tumors. *J Nucl Med* 2016; 57: 708-714.
- [39] Krausz Y, Freedman N, Rubinstein R, Lavie E, Orevi M, Tshori S, Salmon A, Glaser B, Chisin R, Mishani E and J Gross D. <sup>68</sup>Ga-DOTA-NOC PET/CT imaging of neuroendocrine tumors: comparison with <sup>111</sup>In-DTPA-octreotide (OctreoScan(R)). *Mol Imaging Biol* 2011; 13: 583-593.
- [40] Sadowski SM, Neychev V, Millo C, Shih J, Nilubol N, Herscovitch P, Pacak K, Marx SJ and Kebebew E. Prospective study of <sup>68</sup>Ga-DOTATATE positron emission tomography/computed tomography for detecting gastro-enteropancreatic neuroendocrine tumors and unknown primary sites. *J Clin Oncol* 2016; 34: 588-596.
- [41] Van Binnebeek S, Vanbilloen B, Baete K, Terwinghe C, Koole M, Mottaghy FM, Clement PM, Mortelmans L, Bogaerts K, Haustermans K, Nackaerts K, Van Cutsem E, Verslype C, Verbruggen A and Deroose CM. Comparison of diagnostic accuracy of <sup>111</sup>In-pentetreotide SPECT and <sup>68</sup>Ga-DOTATOC PET/CT: a lesion-by-lesion analysis in patients with metastatic neuroendocrine tumours. *Eur Radiol* 2016; 26: 900-909.
- [42] Deppen SA, Blume J, Bobbey AJ, Shah C, Graham MM, Lee P, Delbeke D and Walker RC. <sup>68</sup>Ga-DOTATATE compared with <sup>111</sup>In-DTPA-octreotide and conventional imaging for pulmonary and gastroenteropancreatic neuroen-

## Next generation SSTR PET ligands

- ocrine tumors: a systematic review and meta-analysis. *J Nucl Med* 2016; 57: 872-878.
- [43] Morgat C, Velayoudom-Cephise FL, Schwartz P, Guyot M, Gaye D, Vimont D, Schulz J, Mazere J, Nunes ML, Smith D, Hindie E, Fernandez P and Tabarin A. Evaluation of (68)Ga-DOTA-TOC PET/CT for the detection of duodenopancreatic neuroendocrine tumors in patients with MEN1. *Eur J Nucl Med Mol Imaging* 2016; 43: 1258-1266.
- [44] Srirajaskanthan R, Kayani I, Quigley AM, Soh J, Caplin ME and Bomanji J. The role of <sup>68</sup>Ga-DOT-ATATE PET in patients with neuroendocrine tumors and negative or equivocal findings on <sup>111</sup>In-DTPA-octreotide scintigraphy. *J Nucl Med* 2010; 51: 875-882.
- [45] Werner RA, Bluemel C, Allen-Auerbach MS, Higuchi T and Herrmann K. <sup>68</sup>Gallium- and <sup>90</sup>Yttrium-177Lutetium: "theranostic twins" for diagnosis and treatment of NETs. *Ann Nucl Med* 2015; 29: 1-7.
- [46] Yang J, Kan Y, Ge BH, Yuan L, Li C and Zhao W. Diagnostic role of Gallium-68 DOTATOC and Gallium-68 DOTATATE PET in patients with neuroendocrine tumors: a meta-analysis. *Acta Radiol* 2014; 55: 389-398.
- [47] Poeppel TD, Binse I, Petersenn S, Lahner H, Schott M, Antoch G, Brandau W, Bockisch A and Boy C. <sup>68</sup>Ga-DOTATOC versus <sup>68</sup>Ga-DOT-ATATE PET/CT in functional imaging of neuroendocrine tumors. *J Nucl Med* 2011; 52: 1864-1870.
- [48] Kabasakal L, Demirci E, Ocak M, Decristoforo C, Araman A, Ozsoy Y, Uslu I and Kanmaz B. Comparison of <sup>68</sup>Ga-DOTATATE and <sup>68</sup>Ga-DOTANOC PET/CT imaging in the same patient group with neuroendocrine tumours. *Eur J Nucl Med Mol Imaging* 2012; 39: 1271-1277.
- [49] Wild D, Bomanji JB, Benkert P, Maecke H, Ell PJ, Reubi JC and Caplin ME. Comparison of <sup>68</sup>Ga-DOTANOC and <sup>68</sup>Ga-DOTATATE PET/CT within patients with gastroenteropancreatic neuroendocrine tumors. *J Nucl Med* 2013; 54: 364-372.
- [50] Bozkurt MF, Virgolini I, Balogova S, Beheshti M, Rubello D, Decristoforo C, Ambrosini V, Kjaer A, Delgado-Bolton R, Kunikowska J, Oyen WJG, Chiti A, Giammarile F, Sundin A and Fanti S. Guideline for PET/CT imaging of neuroendocrine neoplasms with <sup>68</sup>Ga-DOTA-conjugated somatostatin receptor targeting peptides and 18F-DOPA. *Eur J Nucl Med Mol Imaging* 2017; 44: 1588-1601.
- [51] Decristoforo C, Pickett RD and Verbruggen A. Feasibility and availability of <sup>68</sup>Ga-labelled peptides. *Eur J Nucl Med Mol Imaging* 2012; 39 Suppl 1: S31-40.
- [52] Velikyan I. <sup>68</sup>Ga-based radiopharmaceuticals: production and application relationship. *Molecules* 2015; 20: 12913-12943.
- [53] Afshar-Oromieh A, Malcher A, Eder M, Eisenhut M, Linhart HG, Hadaschik BA, Holland-Letz T, Giesel FL, Kratochwil C, Haufe S, Haberkorn U and Zechmann CM. PET imaging with a [<sup>68</sup>Ga] gallium-labelled PSMA ligand for the diagnosis of prostate cancer: biodistribution in humans and first evaluation of tumour lesions. *Eur J Nucl Med Mol Imaging* 2013; 40: 486-495.
- [54] Synowiecki MA, Perk LR and Nijssen JFW. Production of novel diagnostic radionuclides in small medical cyclotrons. *EJNMMI Radiopharm Chem* 2018; 3: 3.
- [55] Conti M and Eriksson L. Physics of pure and non-pure positron emitters for PET: a review and a discussion. *EJNMMI Phys* 2016; 3: 8.
- [56] Marciniak A and Brasun J. Somatostatin analogues labeled with copper radioisotopes: current status. *J Radioanal Nucl Chem* 2017; 313: 279-289.
- [57] Boschi A, Martini P, Janevik-Ivanovska E and Duatti A. The emerging role of copper-64 radiopharmaceuticals as cancer theranostics. *Drug Discov Today* 2011; 23: 1489-1501.
- [58] Anderson CJ, Dehdashti F, Cutler PD, Schwarz SW, Laforest R, Bass LA, Lewis JS and McCarthy DW. <sup>64</sup>Cu-TETA-octreotide as a PET imaging agent for patients with neuroendocrine tumors. *J Nucl Med* 2001; 42: 213-221.
- [59] Pfeifer A, Knigge U, Mortensen J, Oturai P, Berthelsen AK, Loft A, Binderup T, Rasmussen P, Elema D, Klausen TL, Holm S, von Benzon E, Hojgaard L and Kjaer A. Clinical PET of neuroendocrine tumors using <sup>64</sup>Cu-DOTATATE: first-in-humans study. *J Nucl Med* 2012; 53: 1207-1215.
- [60] Pfeifer A, Knigge U, Binderup T, Mortensen J, Oturai P, Loft A, Berthelsen AK, Langer SW, Rasmussen P, Elema D, von Benzon E, Hojgaard L and Kjaer A. <sup>64</sup>Cu-DOTATATE PET for neuroendocrine tumors: a prospective head-to-head comparison with <sup>111</sup>In-DTPA-octreotide in 112 patients. *J Nucl Med* 2015; 56: 847-854.
- [61] Johnbeck CB, Knigge U, Loft A, Berthelsen AK, Mortensen J, Oturai P, Langer SW, Elema DR and Kjaer A. Head-to-head comparison of <sup>64</sup>Cu-DOTATATE and <sup>68</sup>Ga-DOTATOC PET/CT: a prospective study of 59 patients with neuroendocrine tumors. *J Nucl Med* 2017; 58: 451-457.
- [62] Hanaoka H, Tominaga H, Yamada K, Paudyal P, Iida Y, Watanabe S, Paudyal B, Higuchi T, Oriuchi N and Endo K. Evaluation of <sup>64</sup>Cu-labeled DOTA-D-Phe1-Tyr 3-octreotide (<sup>64</sup>Cu-DOTA-TOC) for imaging somatostatin receptor-expressing tumors. *Ann Nucl Med* 2009; 23: 559-567.
- [63] Paterson BM, Roselt P, Denoyer D, Cullinane C, Binns D, Noonan W, Jeffery CM, Price RI, White JM, Hicks RJ and Donnelly PS. PET imaging of tumours with a <sup>64</sup>Cu labeled macrobicyclic

## Next generation SSTR PET ligands

- cage amine ligand tethered to Tyr3-octreotate. Dalton Trans 2014; 43: 1386-1396.
- [64] Meisetschlaeger G, Poethko T, Stahl A, Wolf I, Scheidhauer K, Schottelius M, Herz M, Wester HJ and Schwaiger M. Gluc-Lys([<sup>18</sup>F]FP)-TOCA PET in patients with SSTR-positive tumors: biodistribution and diagnostic evaluation compared with [<sup>111</sup>In]DTPA-octreotide. J Nucl Med 2006; 47: 566-573.
- [65] Wieder H, Beer AJ, Poethko T, Meisetschlaeger G, Wester HJ, Rummeny E, Schwaiger M and Stahl AR. PET/CT with Gluc-Lys-([<sup>18</sup>F]FP)-TOCA: correlation between uptake, size and arterial perfusion in somatostatin receptor positive lesions. Eur J Nucl Med Mol Imaging 2008; 35: 264-271.
- [66] Astner ST, Bundschuh RA, Beer AJ, Ziegler SI, Krause BJ, Schwaiger M, Molls M, Grosu AL and Essler M. Assessment of tumor volumes in skull base glomus tumors using Gluc-Lys[<sup>18</sup>F]-TOCA positron emission tomography. Int J Radiat Oncol Biol Phys 2009; 73: 1135-1140.
- [67] Seemann MD. Detection of metastases from gastrointestinal neuroendocrine tumors: prospective comparison of <sup>18</sup>F-TOCA PET, triple-phase CT, and PET/CT. Technol Cancer Res Treat 2007; 6: 213-220.
- [68] Iddon L, Leyton J, Indrevoll B, Glaser M, Robins EG, George AJ, Cuthbertson A, Luthra SK and Aboagye EO. Synthesis and in vitro evaluation of [<sup>18</sup>F]fluoroethyl triazole labelled [Tyr3]octreotate analogues using click chemistry. Bioorg Med Chem Lett 2011; 21: 3122-3127.
- [69] Leyton J, Iddon L, Perumal M, Indrevoll B, Glaser M, Robins E, George AJ, Cuthbertson A, Luthra SK and Aboagye EO. Targeting somatostatin receptors: preclinical evaluation of novel <sup>18</sup>F-fluoroethyltriazole-Tyr3-octreotate analogs for PET. J Nucl Med 2011; 52: 1441-1448.
- [70] Dubash SR, Keat N, Mapelli P, Twyman F, Carroll L, Kozlowski K, Al-Nahhas A, Saleem A, Huiban M, Janisch R, Frilling A, Sharma R and Aboagye EO. Clinical translation of a click-labeled <sup>18</sup>F-octreotate radioligand for imaging neuroendocrine tumors. J Nucl Med 2016; 57: 1207-1213.
- [71] McBride WJ, Sharkey RM, Karacay H, D'Souza CA, Rossi EA, Laverman P, Chang CH, Boerman OC and Goldenberg DM. A novel method of <sup>18</sup>F radiolabeling for PET. J Nucl Med 2009; 50: 991-998.
- [72] Cleeren F, Lecina J, Ahamed M, Raes G, Devoogdt N, Cavelliers V, McQuade P, Rubins DJ, Li W, Verbruggen A, Xavier C and Bormans G. Al<sup>18</sup>F-labeling of heat-sensitive biomolecules for positron emission tomography imaging. Theranostics 2017; 7: 2924-2939.
- [73] Laverman P, D'Souza CA, Eek A, McBride WJ, Sharkey RM, Oyen WJ, Goldenberg DM and Boerman OC. Optimized labeling of NOTA-conjugated octreotide with F-18. Tumor Biol 2012; 33: 427-434.
- [74] Laverman P, McBride WJ, Sharkey RM, Eek A, Joosten L, Oyen WJ, Goldenberg DM and Boerman OC. A novel facile method of labeling octreotide with <sup>18</sup>F-fluorine. J Nucl Med 2010; 51: 454-461.
- [75] Litau S, Niedermoser S, Vogler N, Roscher M, Schirmmayer R, Fricker G, Wangler B and Wangler C. Next generation of SiFAlin-based TATE derivatives for PET imaging of SSTR-positive tumors: influence of molecular design on in vitro SSTR binding and in vivo pharmacokinetics. Bioconjug Chem 2015; 26: 2350-2359.
- [76] Niedermoser S, Chin J, Wangler C, Kostikov A, Bernard-Gauthier V, Vogler N, Soucy JP, McEwan AJ, Schirmmayer R and Wangler B. In vivo evaluation of <sup>18</sup>F-SiFAlin-Modified TATE: a potential challenge for <sup>68</sup>Ga-DOTATATE, the clinical gold standard for somatostatin receptor imaging with PET. J Nucl Med 2015; 56: 1100-1105.
- [77] Wangler C, Waser B, Alke A, Iovkova L, Buchholz HG, Niedermoser S, Jurkschat K, Fottner C, Bartenstein P, Schirmmayer R, Reubi JC, Wester HJ and Wangler B. One-step (<sup>18</sup>F)-labeling of carbohydrate-conjugated octreotate-derivatives containing a silicon-fluoride-acceptor (SiFA): in vitro and in vivo evaluation as tumor imaging agents for positron emission tomography (PET). Bioconjug Chem 2010; 21: 2289-2296.
- [78] Liu Z, Pourghiasian M, Benard F, Pan J, Lin KS and Perrin DM. Preclinical evaluation of a high-affinity <sup>18</sup>F-trifluoroborate octreotate derivative for somatostatin receptor imaging. J Nucl Med 2014; 55: 1499-1505.
- [79] Maschauer S, Heilmann M, Wangler C, Schirmmayer R and Prante O. Radiosynthesis and preclinical evaluation of F-18-fluoroglycosylated octreotate for somatostatin receptor imaging. Bioconjug Chem 2016; 27: 2707-2714.
- [80] Rosch F. Scandium-44: benefits of a long-lived PET radionuclide available from the (44)Ti/(44)Sc generator system. Curr Radiopharm 2012; 5: 187-201.
- [81] van der Meulen NP, Bunka M, Domnanich KA, Muller C, Haller S, Vermeulen C, Turler A and Schibli R. Cyclotron production of (44)Sc: from bench to bedside. Nucl Med Biol 2015; 42: 745-751.
- [82] Muller C, Bunka M, Reber J, Fischer C, Zheronosekov K, Turler A and Schibli R. Promises of cyclotron-produced <sup>44</sup>Sc as a diagnostic match for trivalent beta-emitters: in vitro and in vivo study of a <sup>44</sup>Sc-DOTA-folate conjugate. J Nucl Med 2013; 54: 2168-2174.
- [83] Muller C, Bunka M, Haller S, Koster U, Groehn V, Bernhardt P, van der Meulen N, Turler A and Schibli R. Promising prospects for <sup>44</sup>Sc/<sup>47</sup>Sc-

## Next generation SSTR PET ligands

- based theragnostics: application of  $^{47}\text{Sc}$  for radionuclide tumor therapy in mice. *J Nucl Med* 2014; 55: 1658-1664.
- [84] Muller C, Domnanich KA, Umbricht CA and van der Meulen NP. Scandium and terbium radionuclides for radiotheragnostics: current state of development towards clinical application. *Br J Radiol* 2018; 20180074.
- [85] Pruszyński M, Majkowska-Pilip A, Loktionova NS, Eppard E and Roesch F. Radiolabeling of DOTATOC with the long-lived positron emitter  $^{44}\text{Sc}$ . *Appl Radiat Isot* 2012; 70: 974-979.
- [86] Koumariou E, Pawlak D, Korsak A and Mikolajczak R. Comparison of receptor affinity of  $^{nat}\text{Sc}$ -DOTA-TATE versus  $^{nat}\text{Ga}$ -DOTA-TATE. *Nucl Med Rev Cent East Eur* 2011; 14: 85-89.
- [87] Domnanich KA, Muller C, Farkas R, Schmid RM, Ponsard B, Schibli R, Turler A and van der Meulen NP.  $^{44}\text{Sc}$  for labeling of DOTA- and NODAGA-functionalized peptides: preclinical in vitro and in vivo investigations. *EJNMMI Radiopharm Chem* 2017; 1: 8.
- [88] Rosch F and Baum RP. Generator-based PET radiopharmaceuticals for molecular imaging of tumours: on the way to THERANOSTICS. *Dalton Trans* 2011; 40: 6104-6111.
- [89] Singh A, van der Meulen NP, Muller C, Klette I, Kulkarni HR, Turler A, Schibli R and Baum RP. First-in-human PET/CT imaging of metastatic neuroendocrine neoplasms with cyclotron-produced  $^{44}\text{Sc}$ -DOTATOC: a proof-of-concept study. *Cancer Biother Radiopharm* 2017; 32: 124-132.
- [90] Muller C, Zhernosekov K, Koster U, Johnston K, Dorrer H, Hohn A, van der Walt NT, Turler A and Schibli R. A unique matched quadruplet of terbium radioisotopes for PET and SPECT and for alpha- and beta-radionuclide therapy: an in vivo proof-of-concept study with a new receptor-targeted folate derivative. *J Nucl Med* 2012; 53: 1951-1959.
- [91] Muller C, Vermeulen C, Koster U, Johnston K, Turler A, Schibli R and van der Meulen NP. Alpha-PET with terbium-149: evidence and perspectives for radiotheragnostics. *EJNMMI Radiopharm Chem* 2017; 1: 5.
- [92] Muller C, Vermeulen C, Johnston K, Koster U, Schmid R, Turler A and van der Meulen NP. Pre-clinical in vivo application of  $^{152}\text{Tb}$ -DOTANOC: a radiolanthanide for PET imaging. *EJNMMI Res* 2016; 6: 35.
- [93] Baum RP, Singh A, Benesova M, Vermeulen C, Gnesin S, Koster U, Johnston K, Muller D, Senftleben S, Kulkarni HR, Turler A, Schibli R, Prior JO, van der Meulen NP and Muller C. Clinical evaluation of the radiolanthanide terbium-152: first-in-human PET/CT with  $(^{152}\text{Tb})$ -DOTATOC. *Dalton Trans* 2017; 46: 14638-14646.
- [94] Reubi JC and Maecke HR. Peptide-based probes for cancer imaging. *J Nucl Med* 2008; 49: 1735-1738.
- [95] Smith-Jones PM, Bischof C, Leimer M, Gludovacz D, Angelberger P, Pangerl T, Peck-Radosavljevic M, Hamilton G, Kaserer K, Kofler A, Schlangbauer-Wadl H, Traub T and Virgolini I. DOTA-*lanreotide*: a novel somatostatin analog for tumor diagnosis and therapy. *Endocrinology* 1999; 140: 5136-5148.
- [96] Rodrigues M, Traub-Weidinger T, Leimer M, Li S, Andreae F, Angelberger P, Dudczak R and Virgolini I. Value of  $^{111}\text{In}$ -DOTA-*lanreotide* and  $^{111}\text{In}$ -DOTA-DPhe1-Tyr3-octreotide in differentiated thyroid cancer: results of in vitro binding studies and in vivo comparison with  $^{18}\text{F}$ -FDG PET. *Eur J Nucl Med Mol Imaging* 2005; 32: 1144-1151.
- [97] Rodrigues M, Traub-Weidinger T, Li S, Ibi B and Virgolini I. Comparison of  $^{111}\text{In}$ -DOTA-DPhe1-Tyr3-octreotide and  $^{111}\text{In}$ -DOTA-*lanreotide* scintigraphy and dosimetry in patients with neuroendocrine tumours. *Eur J Nucl Med Mol Imaging* 2006; 33: 532-540.
- [98] Traub-Weidinger T, Von Guggenberg E, Dobrozemsky G, Kendler D, Eisterer W, Bale R, Putzer D, Gabriel M and Virgolini I. Preliminary experience with  $(^{68}\text{Ga})$ -DOTA-*lanreotide* positron emission tomography. *Q J Nucl Med Mol Imaging* 2010; 54: 52-60.
- [99] Putzer D, Kroiss A, Waitz D, Gabriel M, Traub-Weidinger T, Uprimny C, von Guggenberg E, Decristoforo C, Warwitz B, Widmann G and Virgolini IJ. Somatostatin receptor PET in neuroendocrine tumours:  $^{68}\text{Ga}$ -DOTA0,Tyr3-octreotide versus  $^{68}\text{Ga}$ -DOTA0-*lanreotide*. *Eur J Nucl Med Mol Imaging* 2013; 40: 364-372.
- [100] Demirci E, Ocak M, Kabasakal L, Araman A, Ozsoy Y and Kanmaz B. Comparison of  $^{68}\text{Ga}$ -DOTA-TATE and  $^{68}\text{Ga}$ -DOTA-LAN PET/CT imaging in the same patient group with neuroendocrine tumours: preliminary results. *Nucl Med Commun* 2013; 34: 727-732.
- [101] Traub-Weidinger T, Putzer D, von Guggenberg E, Dobrozemsky G, Nilica B, Kendler D, Bale R and Virgolini IJ. Multiparametric PET imaging in thyroid malignancy characterizing tumour heterogeneity: somatostatin receptors and glucose metabolism. *Eur J Nucl Med Mol Imaging* 2015; 42: 1995-2001.
- [102] Ginj M, Zhang H, Eisenwiener KP, Wild D, Schulz S, Rink H, Cescato R, Reubi JC and Maecke HR. New pansomatostatin ligands and their chelated versions: affinity profile, agonist activity, internalization, and tumor targeting. *Clin Cancer Res* 2008; 14: 2019-2027.
- [103] Fani M, Mueller A, Tamma ML, Nicolas G, Rink HR, Cescato R, Reubi JC and Maecke HR. Radiolabeled bicyclic somatostatin-based ana-

## Next generation SSTR PET ligands

- logs: a novel class of potential radiotracers for SPECT/PET of neuroendocrine tumors. *J Nucl Med* 2010; 51: 1771-1779.
- [104] Tatsi A, Maina T, Cescato R, Waser B, Krenning EP, de Jong M, Cordopatis P, Reubi JC and Nock BA. [<sup>111</sup>In-DOTA]Somatostatin-14 analogs as potential pansomatostatin-like radiotracers-first results of a preclinical study. *EJNMMI Res* 2012; 2: 25.
- [105] Maina T, Cescato R, Waser B, Tatsi A, Kaloudi A, Krenning EP, de Jong M, Nock BA and Reubi JC. [<sup>111</sup>In-DOTA]LTT-SS28, a first pansomatostatin radioligand for in vivo targeting of somatostatin receptor-positive tumors. *J Med Chem* 2014; 57: 6564-6571.
- [106] Bruns C, Lewis I, Briner U, Meno-Tetang G and Weckbecker G. SOM230: a novel somatostatin peptidomimetic with broad somatotropin release inhibiting factor (SRIF) receptor binding and a unique antisecretory profile. *Eur J Endocrinol* 2002; 146: 707-716.
- [107] Liu F, Liu T, Xu X, Guo X, Li N, Xiong C, Li C, Zhu H and Yang Z. Design, synthesis, and biological evaluation of <sup>68</sup>Ga-DOTA-PA1 for lung cancer: a novel PET tracer for multiple somatostatin receptor imaging. *Mol Pharm* 2018; 15: 619-628.
- [108] Tian R, Jacobson O, Niu G, Kiesewetter DO, Wang Z, Zhu G, Ma Y, Liu G and Chen X. Evans blue attachment enhances somatostatin receptor subtype-2 imaging and radiotherapy. *Theranostics* 2018; 8: 735-745.
- [109] Zhang J, Wang H, Jacobson Weiss O, Cheng Y, Niu G, Li F, Bai C, Zhu Z and Chen X. Safety, pharmacokinetics and dosimetry of a long-acting radiolabeled somatostatin analogue (<sup>177</sup>Lu-DOTA-EB-TATE) in patients with advanced metastatic neuroendocrine tumors. *J Nucl Med* 2018.
- [110] Gjinj M, Zhang H, Waser B, Cescato R, Wild D, Wang X, Erchegyi J, Rivier J, Macke HR and Reubi JC. Radiolabeled somatostatin receptor antagonists are preferable to agonists for in vivo peptide receptor targeting of tumors. *Proc Natl Acad Sci U S A* 2006; 103: 16436-16441.
- [111] Bodei L and Weber WA. Somatostatin receptor imaging of neuroendocrine tumors: from agonists to antagonists. *J Nucl Med* 2018; 59: 907-908.
- [112] Wild D, Fani M, Behe M, Brink I, Rivier JE, Reubi JC, Maecke HR and Weber WA. First clinical evidence that imaging with somatostatin receptor antagonists is feasible. *J Nucl Med* 2011; 52: 1412-1417.
- [113] Fani M, Nicolas GP and Wild D. Somatostatin receptor antagonists for imaging and therapy. *J Nucl Med* 2017; 58: 61S-66S.
- [114] Fani M, Braun F, Waser B, Beetschen K, Cescato R, Erchegyi J, Rivier JE, Weber WA, Maecke HR and Reubi JC. Unexpected sensitivity of sst2 antagonists to N-terminal radiometal modifications. *J Nucl Med* 2012; 53: 1481-1489.
- [115] Nicolas GP, Beykan S, Bouterfa H, Kaufmann J, Bauman A, Lassmann M, Reubi JC, Rivier JEF, Maecke HR, Fani M and Wild D. Safety, biodistribution, and radiation dosimetry of (<sup>68</sup>Ga-OPS202) in patients with gastroenteropancreatic neuroendocrine tumors: a prospective phase I imaging study. *J Nucl Med* 2018; 59: 909-914.
- [116] Nicolas GP, Schreiter N, Kaul F, Uiters J, Bouterfa H, Kaufmann J, Erlanger TE, Cathomas R, Christ E, Fani M and Wild D. Sensitivity comparison of (<sup>68</sup>Ga-OPS202) and (<sup>68</sup>Ga-DOTA-TOC) PET/CT in patients with gastroenteropancreatic neuroendocrine tumors: a prospective phase II imaging study. *J Nucl Med* 2018; 59: 915-921.
- [117] Sandstrom M, Velikyan I, Garske-Roman U, Sorensen J, Eriksson B, Granberg D, Lundqvist H, Sundin A and Lubberink M. Comparative biodistribution and radiation dosimetry of <sup>68</sup>Ga-DOTATOC and <sup>68</sup>Ga-DOTATATE in patients with neuroendocrine tumors. *J Nucl Med* 2013; 54: 1755-1759.
- [118] Dalm SU, Nonnekens J, Doeswijk GN, de Blois E, van Gent DC, Konijnenberg MW and de Jong M. Comparison of the therapeutic response to treatment with a <sup>177</sup>Lu-labeled somatostatin receptor agonist and antagonist in preclinical models. *J Nucl Med* 2016; 57: 260-265.
- [119] Nicolas GP, Mansi R, McDougall L, Kaufmann J, Bouterfa H, Wild D and Fani M. Biodistribution, pharmacokinetics, and dosimetry of (<sup>177</sup>Lu-, (<sup>90</sup>Y-, and (<sup>111</sup>In)-labeled somatostatin receptor antagonist OPS201) in comparison to the agonist (<sup>177</sup>Lu-DOTATATE): the mass effect. *J Nucl Med* 2017; 58: 1435-1441.
- [120] Wild D, Fani M, Fischer R, Del Pozzo L, Kaul F, Krebs S, Rivier JE, Reubi JC, Maecke HR and Weber WA. Comparison of somatostatin receptor agonist and antagonist for peptide receptor radionuclide therapy: a pilot study. *J Nucl Med* 2014; 55: 1248-1252.
- [121] Dalm SU, Haeck J, Doeswijk GN, de Blois E, de Jong M and van Deurzen CHM. SSTR-mediated imaging in breast cancer: is there a role for radiolabeled somatostatin receptor antagonists? *J Nucl Med* 2017; 58: 1609-1614.
- [122] Cescato R, Waser B, Fani M and Reubi JC. Evaluation of <sup>177</sup>Lu-DOTA-sst2 antagonist versus <sup>177</sup>Lu-DOTA-sst2 agonist binding in human cancers in vitro. *J Nucl Med* 2011; 52: 1886-1890.
- [123] Reubi JC, Waser B, Macke H and Rivier J. Highly increased 125I-JR11 antagonist binding in vitro reveals novel indications for sst2 target-

## Next generation SSTR PET ligands

- ing in human cancers. *J Nucl Med* 2017; 58: 300-306.
- [124] Dude I, Zhang Z, Rousseau J, Hundal-Jabal N, Colpo N, Merkens H, Lin KS and Benard F. Evaluation of agonist and antagonist radioligands for somatostatin receptor imaging of breast cancer using positron emission tomography. *EJNMMI Radiopharm Chem* 2017; 2: 4.
- [125] Wester HJ, Schottelius M, Scheidhauer K, Meisetschlager G, Herz M, Rau FC, Reubi JC and Schwaiger M. PET imaging of somatostatin receptors: design, synthesis and preclinical evaluation of a novel <sup>18</sup>F-labelled, carbohydrate analogue of octreotide. *Eur J Nucl Med Mol Imaging* 2003; 30: 117-122.